AN EXPERIMENTAL STUDY OF AERODYNAMIC FORCES OF AIR BARS

By

SAI KISHORE V. NISANKARARAO

Bachelor of Engineering

Madras University

Madras, India

1991

Submitted to the Faculty of the
Graduate College of the
Oklahoma State University
in partial fulfillment of
the requirements for
the Degree of
MASTER OF SCIENCE
May, 1994

OKLAHOMA STATE UNIVERSITY

AN EXPERIMENTAL STUDY OF

AERODYNAMIC FORCES

OF AIR BARS

Thesis Approved:

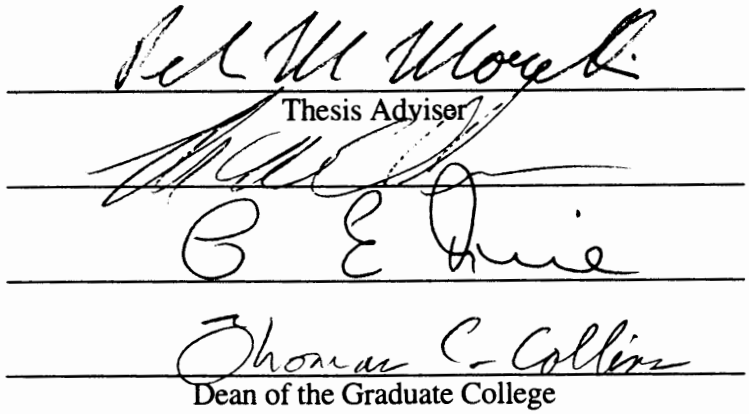

Thesis Adviser

Dean of the Graduate College

ACKNOWLEDGMENTS

I would like to thank Dr. Peter M. Moretti for serving as my advisor during this work. I am deeply indebted to him for the constant encouragement and unflinching support he has provided me. I would also like to thank Dr. Chambers and Dr. Price for agreeing to serve on my committee. Special thanks are also due to Dr. Chambers for sharing laboratory equipment with me.

My special thanks go to Dr. Young Bae Chang for his exceptional and consistent guidance during every stage of my project irrespective of time and place.

TABLE OF CONTENTS

Chapter		Page
I. INTRODUCTION		1
II. LITERATURE REVIEW		3
	2.1 Air-Flotation System	3
	2.2 Air-Flotation drying	4
	2.3 Design Features	7
III. EXPERIMENTAL PROCEDURE		11
IV. RESULTS AND DISCUSSION		17
	4.1 Aerodynamic Forces with Uniform Flotation Height	17
	4.1.1 Airfoil Air Bar	17
	4.1.2 Pressure Pad Tube, Width is 3.6"	23
	4.1.3 Pressure Pad Tube, Width is 5.0"	28
	4.1.4 Comparison with Ground-Effect Theory	33
	4.2 Effects of Cross-Machine-Directional Tilt Angle	37
	4.2.1 Pressure Pad Tube, Width is 5.0", Holes Closed	38
V. SUMMARY AND CONCLUSIONS		45
CITED WORKS		47

LIST OF FIGURES

Figure	Page
1. Web Supported by Air Bars in a Flotation Oven	4
2. Model of Ground-Effect Machine	5
3. Different Types of Air Bars	8
4. Graph Developed by Fraser Showing The Relationship Between Heat Transfer Coefficient and Tube Spacing	9
5. Web Supported by Spaced Air Bars in Flotation Ovens	9
6. Web Supported by Over-Lapping Air Bars in Flotation Ovens	10
7. Front View of the Test Setup	11
8. Side View of the Test Setup	12
9. Air Bar A (Pressure Pad Tube, Slot-to-Slot Width is 3.6", Center Holes Closed)	13
10. Air Bar B (Pressure Pad Tube, Slot-to-Slot Width is 3.6", Center Holes Open)	14
11. Air Bar C (Pressure Pad Tube, Slot-to-Slot Width is 5.0", Center Holes Open)	14
12. Air Bar D (Pressure Pad Tube, Slot-to-Slot Width is 5.0", Center Holes Closed)	15
13. Air Bar E (Air Foil Air Bar with Trailing Edge Slots Open)	15
14. Pressure Distribution of Air Foil (Trailing Edge Slot Open), Gap is 0.03"	18
15. Pressure Distribution of Air Foil (Trailing Edge Slot Open), Gap is 0.05"	18
16. Pressure Distribution of Air Foil (Trailing Edge Slot Open), Gap is 0.07"	19
17. Pressure Distribution of Air Foil (Trailing Edge Slot Open), Gap is 0.10"	19

Figure Page

18. Pressure Distribution of Air Foil (Trailing Edge Slot Open) for Two Setups, Gap is 0.03" 20

19. Pressure Distribution of Air Foil (Trailing Edge Slot Open) for Two Setups, Gap is 0.05" 21

20. Pressure Distribution of Air Foil (Trailing Edge Slot Open) for Two Setups, Gap is 0.07" 21

21. Comparison of Lift Forces for Air Foil Air Bar (Trailing Edge Slots Open) 22

22. Effect of Gap on Pressure for Pressure Pad Tube, Width is 3.6", Center Holes Closed, Gap = 0.03" 24

23. Effect of Gap on Pressure for Pressure Pad Tube, Width is 3.6", Center Holes Closed, Gap = 0.05" 25

24. Effect of Gap on Pressure for Pressure Pad Tube, Width is 3.6", Center Holes Closed, Gap = 0.10" 25

25. Effect of Gap on Pressure for Pressure Pad Tube, Width is 3.6", Center Holes Closed, Gap = 0.20" 26

26. Effect of Gap on Pressure for Pressure Pad Tube, Width is 3.6", Center Holes Open, Gap = 0.036" 26

27. Effect of Gap on Pressure for Pressure Pad Tube, Width is 3.6", Center Holes Open, Gap = 0.07" 27

28. Effect of Gap on Pressure for Pressure Pad Tube, Width is 3.6", Center Holes Open, Gap = 10" 27

29. Comparison of Lift Forces for Pressure Pad Tube, Width is 3.6" 28

30. Effect of Gap on Pressure for Pressure Pad Tube, Width is 5.0", Center Holes Open, Gap = 0.03" 29

31. Effect of Gap on Pressure for Pressure Pad Tube, Width is 5.0", Center Holes Open, Gap = 0.05" 30

32. Effect of Gap on Pressure for Pressure Pad Tube, Width is 5.0", Center Holes Open, Gap = 0.10" 30

33. Effect of Gap on Pressure for Pressure Pad Tube, Width is

Figure Page

5.0", Center Holes Open, Gap = 0.20" 31

34. Effect of Gap on Pressure for Pressure Pad Tube, Width is 5.0", Center Holes Closed, Gap = 0.03" 31

35. Effect of Gap on Pressure for Pressure Pad Tube, Width is 5.0", Center Holes Closed, Gap = 0.05" 32

36. Effect of Gap on Pressure for Pressure Pad Tube, Width is 5.0", Center Holes Closed, Gap = 0.10" 32

37. Effect of Gap on Pressure for Pressure Pad Tube, Width is 5.0", Center Holes Closed, Gap = 0.20" 33

38. Comparison of Lift Forces for Pressure Pad Tube, Width is 5.0" 33

39. Equivalent Values of S, b and h are Shown 34

40. Horizontal Position of Peak Pressure for Various Flotation Heights 35

41. Variation of P_c (Theoretical) with Flotation Height 36

42. Variation of Theoretical Lift Force with Flotation Height 36

43. Comparison of Theoretical and Experimental Values of Pressure 37

44. Comparison of Theoretical and Experimental Values of Force 37

45. Setup for Cross-Machine-Directional Tilt Angle 38

46. Variation of Pressure with Local Gap for Pressure Pad Tube, Width is 5.0", Tilt Angle is 0.77° 39

47. Variation of Pressure with Local Gap for Pressure Pad Tube, Width is 5.0", Tilt Angle is 0.63° 40

48. Variation of Pressure with Local Gap for Pressure Pad Tube, Width is 5.0", Tilt Angle is 0.49° 40

49. Variation of Pressure with Local Gap for Air Foil, Tilt Angle is 0.79° 41

50. Variation of Pressure with Local Gap for Air Foil, Tilt Angle is 0.51° 41

51. Comparison of Pressure Forces for Two Cases For Pressure Pad Tube, Width is 5.0", Tilt Angle is 0.77° 42

Figure Page

52. Comparison of Pressure Forces for Two Cases for Pressure Pad Tube, Width is 5.0", Tilt Angle is 0.63° 43

53. Variation of Pressure with Local Gap for Air Foil, Tilt Angle is 0° 43

54. Variation of Pressure with Local Gap for Pressure Pad Tube, Width is 5.0", Center Holes Closed, Tilt Angle is 0° 44

NOMENCLATURE

b	Thickness of jet flow (width of jet exit)
F	Resultant aerodynamic force per unit width of web
h	Gap between the web and the air bar
P_c	Constant pressure developed in the gap between the air bar and the web
P_j	Peak pressure
P_s	Supply pressure
PPT	Pressure Pad Tube
S	Distance from the edge of the slot to the surface of the air bar
V_{jet}	Velocity of the jet flow
w	Width of the air bar (Distance between the two nozzles)
ø	Angle of jet flow at the exit
e	Air density

CHAPTER I

INTRODUCTION

A web is a thin, continuous and flexible material such as paper, film or fabric. Prior to being converted to a final product, a web goes through various processes such as coating, drying and laminating. In many web-handling processes, substantial lengths of moving webs are supported by air bars. A web has to go through the process of drying when it is coated. Drying of a web may be carried out in a flotation oven by the impingement of heated air from both the top and bottom of the web.

The reaction of the air jets on the web may produce a lateral force. If this lateral force is big enough, it may displace the web, cause flutter or damage the coating.

Pinnamaraju (1992), utilized static web experiments. Several industrial air bars were used and a web was modeled as a rigid Lucite plate. The total lift forces were measured as a function of the flotation height between the airbar and the web. A comparison of lift forces was made from various air bars. The lift forces were positive for a wide range of gaps for all the air bars except the airfoil type air bar. It is indicated that the airfoil type air bar with vented slots can only be used at small flotation heights (less than 0.05 inch) due to loss of lift on the web. Also, this air bar exhibited strong stability over the range of small flotation heights.

Pinnamaraju (1992) pointed out that on a lift force versus gap spacing graph, a negative slope is a stable characteristic. When the gap spacing is very small, the large negative slope would act like a very stiff spring to keep the web from touching the surface

of the air bar. As the gap spacing increases, the spring stiffness between the web and air bar decreases.

Static web experiments are continued using the same air bars that were used by Pinnamaraju. These experiments attempt to test the replicability of the results obtained in the experiments conducted by Pinnamaraju. Also, experiments are performed to check the effect of cross machine directional (CMD) tilt of the rigid plate, which is hypothesized to be the cause of lateral instability of a web moving in a flotation oven. A comparison will be made between the results for uniform flotation height and CMD tilt of the rigid plate. The measured pressure distributions and the total aerodynamic forces on the rigid web will be compared with the ground effect theory.

CHAPTER II

LITERATURE REVIEW

2.1 Air-Flotation System

Flotation systems are widely used in the drying of paper, film and fabric webs. It is well known that a boundary layer exists at the interface of a web and a flotation system. A boundary layer has low conductivity to heat transfer into a web and also high resistance to mass transport of vapor away from the web surface. So, the idea is to use high-velocity fluid to dissipate this boundary layer as quickly as possible, and transfer energy to the surface of the web for rapid drying and transportation of the web.

According to Obrzut (1976), the primary part of a flotation system is an air bar. An air bar is actually a pressure chamber with continuous slotted openings extending across the full width of the web. Figure 1 shows a web supported by air bars in a flotation oven. High-velocity air is forced through the slotted openings, which exerts a pressure force between the air bar and web. The web acts as a physical barrier and the pressure force pushes the web from the surface of the air bar. Using a single air bar results in unstable flotation since, the pressure force would push the web away until the lift forces equaled the weight of the web. The web would then drop until the pressure force once again increased to push the web away from the air bar. Stability can be achieved by placing an air bar of similar design in a staggered position on the opposite side of the web.

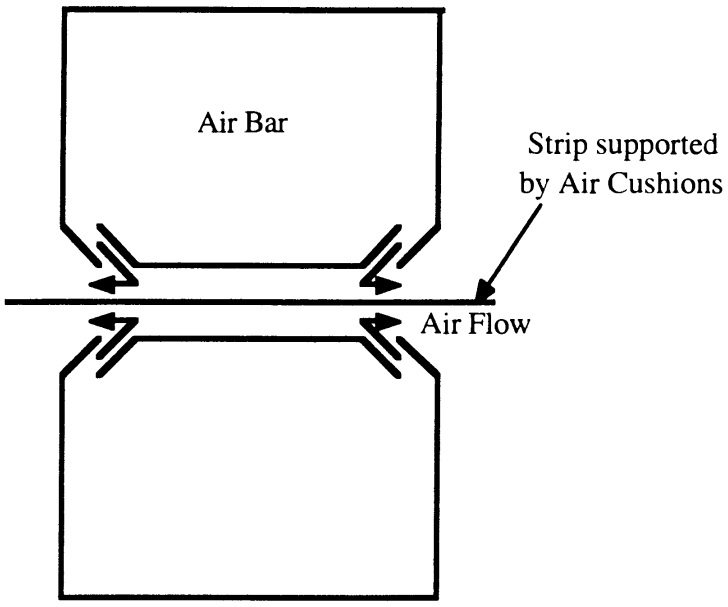

Figure 1. Web Supported by Air Bars in Flotation Oven

According to Obrzut (1976), symmetry of flow is accomplished by supplying each nozzle from both ends and uniformly exhausting air from the center of the web's path. Also, bowed and cambered webs with wavy edges present no problem for flotation systems. One of the important features of a flotation system is the flattening effect on bowed or crowned webs. The reason is that the web closest to the air bar is subjected to the highest pressure forces which, in turn, tends to push the web to its stable position between the air bars.

2.2 Air-Flotation Drying

Fraser (1983) determined in drying a web that there are three over-lapping phases. The first phase is the sensible heat build-up phase, where the web is brought to the proper

drying temperature. The second phase is the constant evaporation rate phase, where most of the solvent evaporates and drying of the web occurs. The third phase is the falling evaporation rate phase, where the last of the solvent is evaporated and the temperature of the web and coating are brought back to a normal temperature.

Also, Fraser (1983) determined that there are two distinct phases to the drying of coatings on webs. The first phase deals with the heat transmitted to the web and a corresponding mass transfer. The mass transfer is the dissipation of the wet boundary layer to the atmosphere. The second phase deals with the migration of the solvent, through the resin or coating, to the surface of the web which is exposed to the atmosphere.

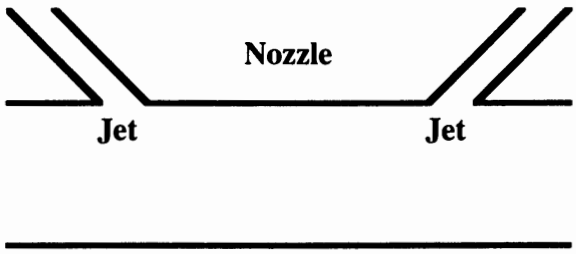

Figure 2. Model of Ground Effect Machine

Davies and Wood (1983) studied the aerodynamics of ground-effect machines, as schematically shown in Figure 2. They showed that the force acting on the plate was proportional to the momentum flux of the jets, but was roughly inversely proportional to the flotation height. Also, they showed that a static strip will float at a height where the weight and the force due to the upper air bar balances the force due to the lower air bar. This balance will not be achieved if the air bar consists of a single jet only, as the force acting on the plate would be independent of the flotation height. In actual flotation

systems, the ratio of web speed to nozzle exit speed is much less than one, thus justifying the use of a stationary strip model.

Based on the ground-effect machine theory, the pressure developed between the flotation device and the wall is

$$P_c / P_j = 2\,ß /(1 + ß) \quad (1)$$

where P_j is the total pressure of the jet flow at the exit, and

$$ß = b\frac{(1+\cos ø)}{h} \quad (2)$$

Equation (2) indicates that ß must be smaller than one, otherwise the pressure developed between the wall and the flotation device is greater than the total pressure of the air jet violating the physical law. For the case of a small flotation height where ß is greater than one, the following equation can be used (Mair, 1964):

$$P_c / P_j = 1 - \exp^{-2ß} \quad (3)$$

The aerodynamic force on the unit width of the wall is

$$F = P_c w + 2\,e\,b\,V^2_{jet} \sin ø \quad (4)$$

Details of these equations are discussed in Moretti and Chang (1994).

Kataoka (1985) has shown that a round free jet issuing from a circular convergent nozzle and impinging normally on a flat plate is influenced by nozzle-to-plate spacing. For a small nozzle-to-plate spacing, the free jet impinges on the flat plate with loss of its initial velocity before it becomes developed. For a large nozzle-to-plate spacing, the free jet becomes fully developed before it impinges on the plate. In the fully developed region, the jet velocity decreases inversely with the distance between nozzle exit and plate. It was also shown that if the jet is isothermal, except in the boundary layer on the flat plate where heat transfer takes place, the optimal impingement spacing to maximize heat transfer is between six and eight nozzle diameters. It was also shown that the optimal spacing is the nozzle-to-plate spacing at which the stagnation point heat flux becomes a maximum.

When a fluid is flowing past an immersed body, and at a point on the body if the resultant velocity becomes zero, the values of pressure, temperature and density at that

point are called stagnation properties. The point is called the stagnation point. The values of pressure, density and temperature are called stagnation pressure, stagnation density and stagnation temperature respectively.

Hwang and Liu (1989) showed that for small gaps between a planar jet with a flat upper surface and a wall, the static pressure at the stagnation point is high. The ground plane pressures on either side of the stagnation point are below ambient. So a strong acceleration in the impingement flow occurs due to the lower pressures on either side of the stagnation point.

2.3 Design Features

According to Fraser (1983), different types of air bars are the arch dryer, sinusoidal tube and the airfoil tube (Figure 3). In the arch dryer, the distance between the nozzle and web ranges from 1.75 to 2.5 inches. The nozzles are about 6 inches apart. The effective velocity at the web surface and the effective length over which the velocity works is markedly reduced because of this wide spacing. As a result, there is a waste of expended energy. In the case of sinusoidal and airfoil tubes, the gap between the nozzle and web is greatly reduced. This increases the effective velocity at the web surface and the effective length over which the velocity acts is greatly increased. All this leads to an appreciably increased heat-transfer coefficient. Theoretically, an airfoil tube has a slightly higher heat-transfer coefficient because of the Bernoulli principle, which governs its operation. The Bernoulli effect causes the web to be drawn towards the surface of the air bar, which in turn increases the air velocity. Air foil tubes tend to exhibit better directional stability because a single directional force tends to keep the web in a straight line. Sinusoidal tubes have minor variation in their design features depending on the manufacturer. They generally have two end nozzles directing the air towards the center of the air bar to give a lift to the web and counteract the Bernoulli effect.

According to Fraser (1983), any web that stretches due to the action of heat or mechanical instability should never be handled by an air-float system. In addition to the tube design, the next important aspect for optimum heat transfer is tube spacing. Tube spacing is the center line distance between each tube measured bottom to bottom or top to top.

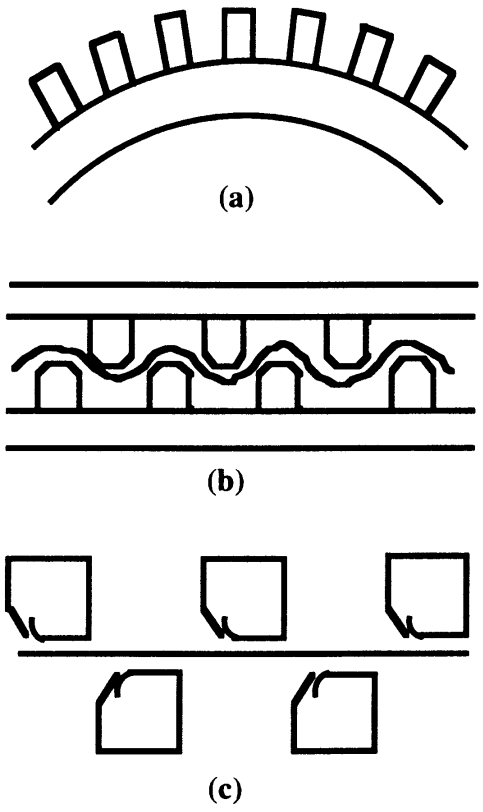

Figure 3. a. Conventional Air Impingement Nozzles of an Arch Dryer

b. Sinusoidal Web Path Pressure-Pads on Each Side of the Web

c. Air Foil Tubes on Each Side of the Web

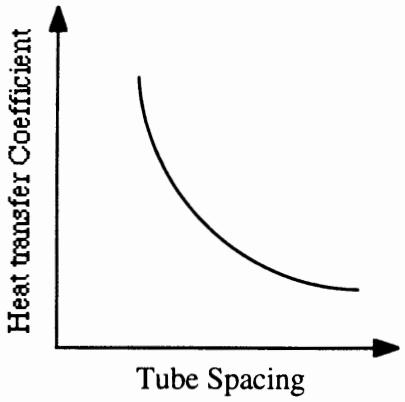

Figure 4. Graph Developed by Fraser Showing the Relationship between Heat Transfer Coefficient and Tube Spacing

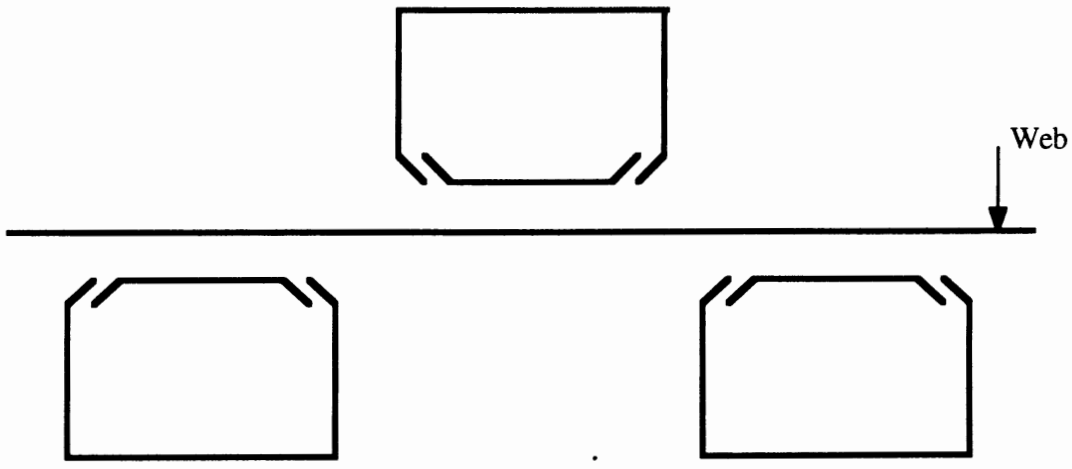

Figure 5. Web Supported by Spaced Air Bars in Flotation Ovens

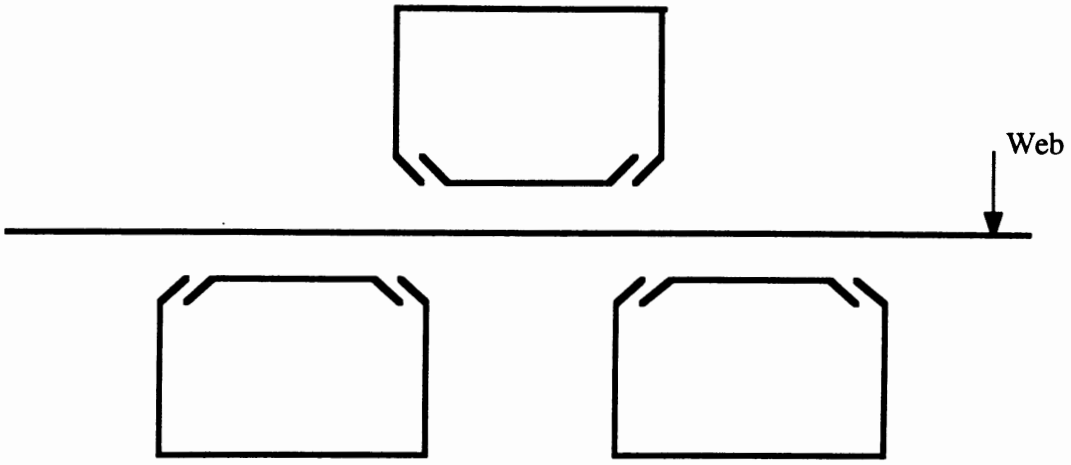

Figure 6. Web Supported by Overlapping Air Bars in Flotation Ovens

Closer tube spacing results in a higher heat-transfer coefficient. In drying some types of coatings, the migration rate of the solvent to the outer surface of the web occurs at a fixed rate. So increasing the heat-transfer rate can have adverse effects, such as bubbles and blisters. Excessive gaps between the surfaces of the top and bottom air bars, with some webs, cause flutter or bounce. The spacing of air bars should not overlap. This has been proven to be unacceptable in past oven designs (Fraser, 1983). The combination between the type of web, the unsupported length to web width ratio, and the web tension can cause lateral web instability.

According to Page and Seyed-Yagoobi (1990), turbulent impinging jets can be used for all practical purposes of drying. These jets produce heat and mass transfer coefficients that are closely coupled. The fluids used in the impinging jet may be gaseous or liquid. The impingement, which is directed by a nozzle, may occur in an environment of the same fluid as that of the jet, this is referred to as a "submerged" jet impingement. On the other hand, it may occur in an environment of a different fluid, which is referred to as a "free" jet impingement.

CHAPTER III

EXPERIMENTAL PROCEDURE

The following diagrams show the setup that was used to perform the experiments on air bars of different geometries.

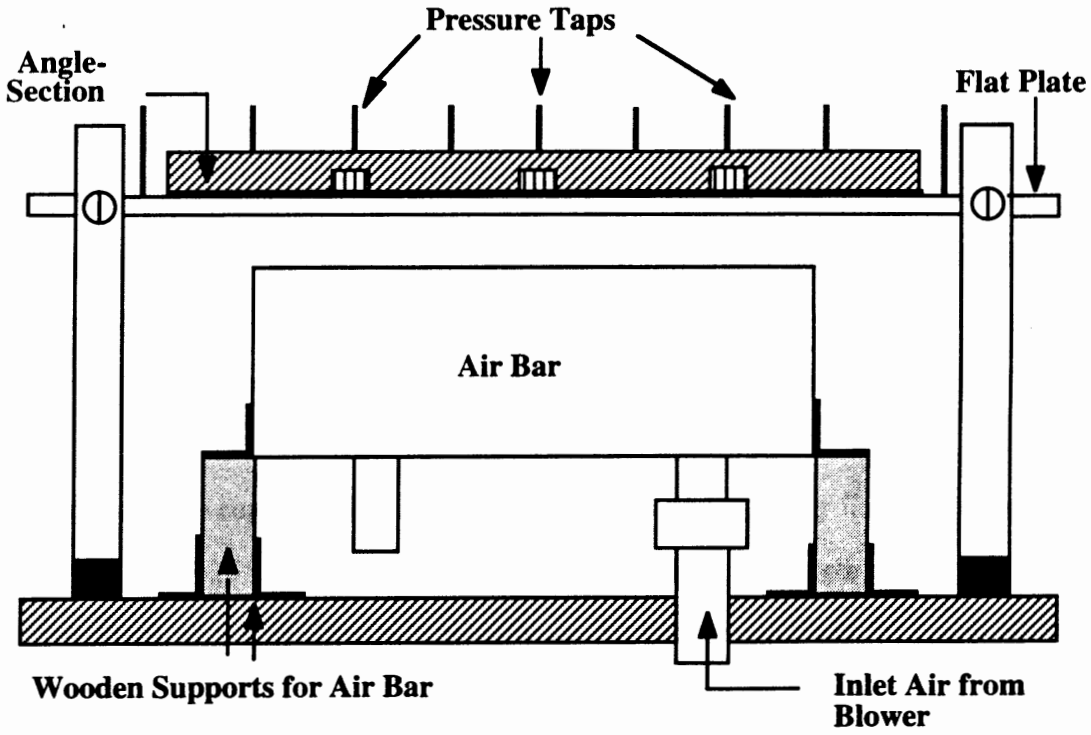

Figure 7. Front View of the Test Setup

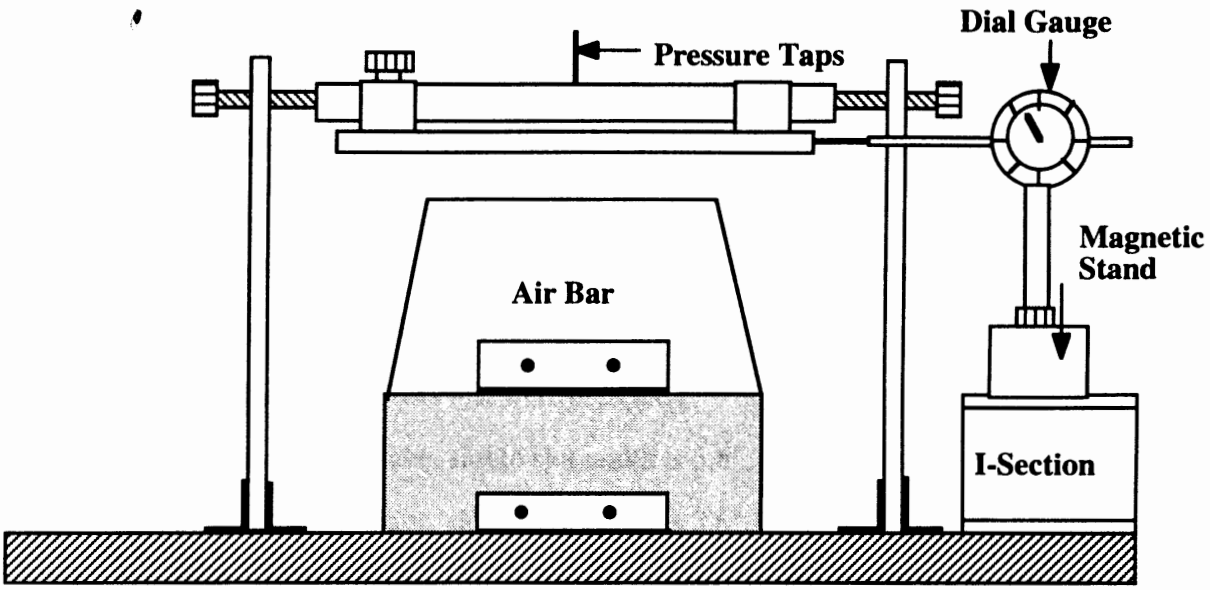

Figure 8. Side View of the Test Setup

As seen from the figures, the air bar is mounted on two wooden supports and is fixed firmly. The flat plate is supported on four steel columns, using two smooth circular steel rods. The flat plate can be moved back and forth on these steel rods. The ends of the steel rods are provided with threaded screws and nuts. The top half of the columns are provided with slots so that the flat plate can be fixed at various heights. The bending of the plate was prevented by fixing two steel stiffeners along the length of the plate.

The gap between the plate and the air bar was varied using feeler gauges. Pressure taps of 0.0625 inch in diameter were installed along the length of the plate. The pressure taps were connected to a manometer that has a resolution of 0.1 inch of water. Taking pressure reading in the machine direction required that the plate be moved by hand, while monitoring the distance moved in the machine direction with a dial gauge indicator having a resolution of 0.001 inch.

The air was supplied by a blower that has a capacity of 580 cfm at zero pressure load. Flow rate was not controlled. It is seen that the plate is parallel to the air bar by insuring the pressure distributions along the length of the air bar were nearly the same. For each longitudinal position, the pressure on the plate was read off the manometer in inches of water.

While checking the effect of cross machine directional tilt, pressure on the plate was read off nine pressure taps along the length of the plate.

The geometries of air bars that were used are :

(1) Air Bar A (Pressure pad tube, slot to slot width is 3.6", center holes closed).

(2) Air Bar B (Pressure pad tube, slot to slot width is 3.6", center holes open).

(3) Air Bar C (Pressure pad tube, slot to slot width is 5.0", center holes open).

(4) Air Bar D (Pressure pad tube, slot to slot width is 5.0", center holes closed).

(5) Air Bar E (Airfoil air bar with trailing edge slots open).

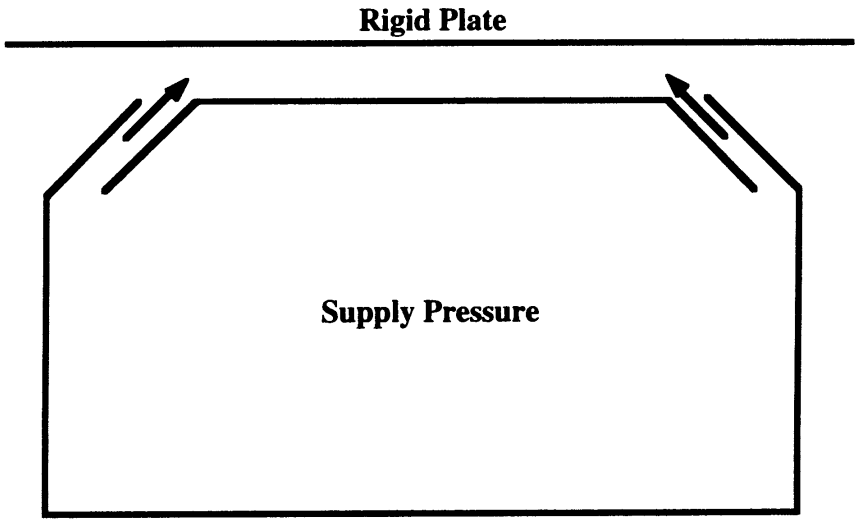

Figure 9. Air Bar A (Pressure Pad Tube, Slot-to-Slot Width is 3.6", Center Holes Closed)

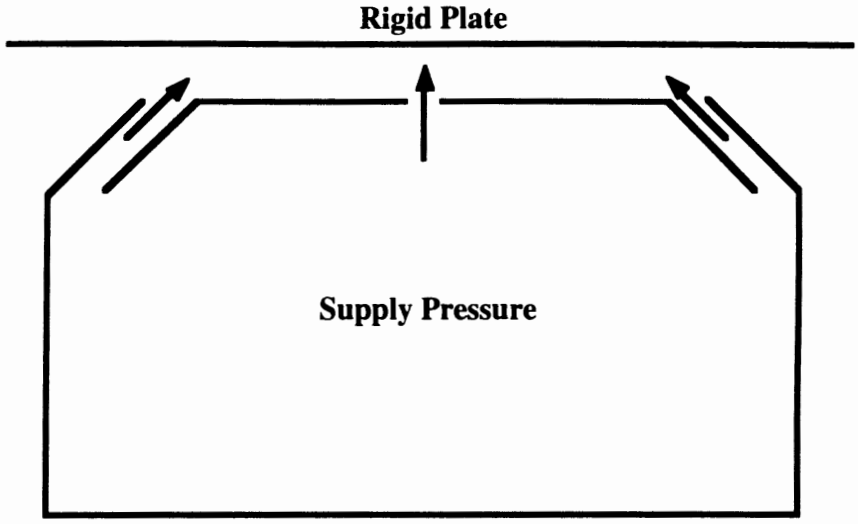

Figure 10 Air Bar B (Pressure Pad Tube, Slot-to-Slot width is 3.6",Center Holes Open)

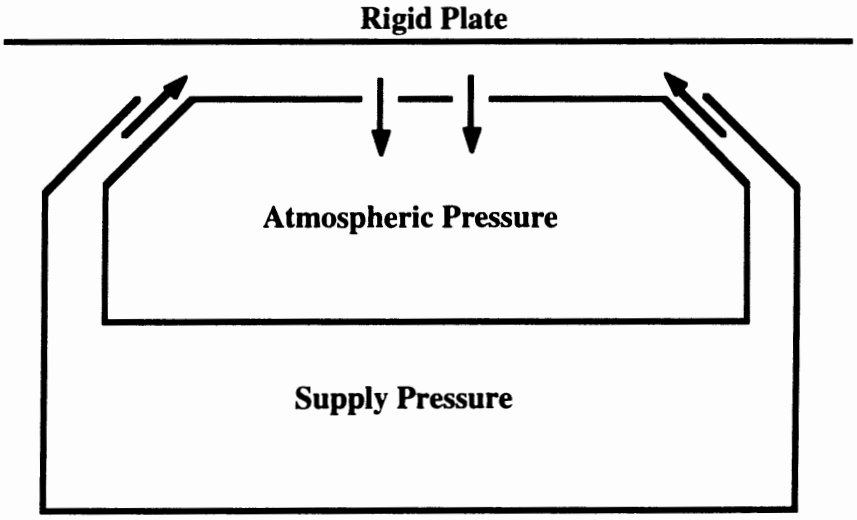

Figure11. Air Bar C (Pressure Pad Tube, Slot-to-Slot Width is 5.0", Center Holes Open)

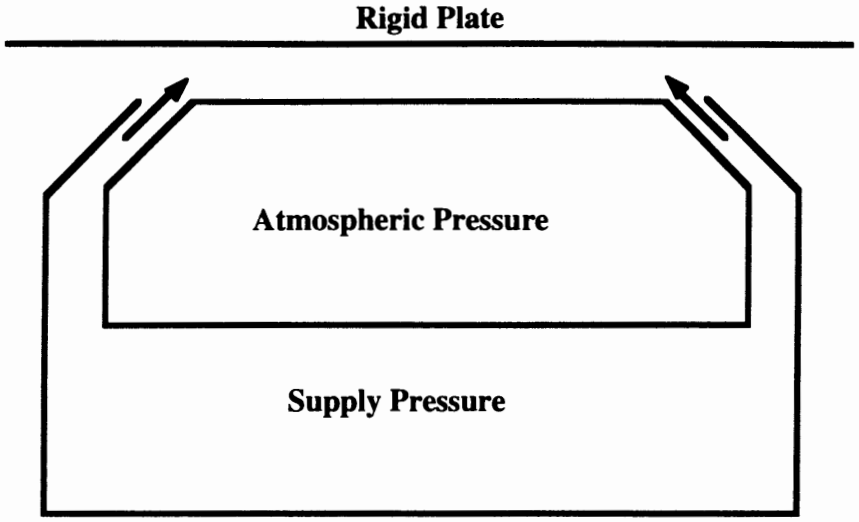

Figure12. Air Bar D (Pressure Pad Tube, Slot-to-Slot Width is 5.0", Center Holes Closed)

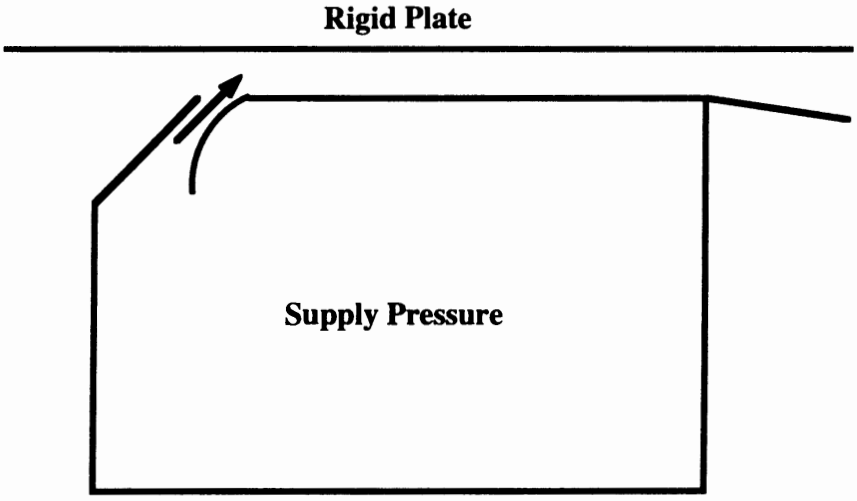

Figure 13. Air Bar E (Airfoil Air Bar with Trailing Edge Slots Open)

For the pressure pad tubes, the pressure readings were taken from the center of the air bar to the slot out to the point where the manometer reads the atmospheric pressure. For the airfoil air bar the measurement was from the center of the slot .

CHAPTER IV

RESULTS AND DISCUSSION

4.1 Aerodynamic Forces with Uniform Flotation Height

4.1.1 Airfoil Air Bar

For the airfoil air bar, pressure readings were taken from the center of the slot, along the width of the air bar, until the manometer read the atmospheric pressure. Four sets of feeler gauges were placed along the length of the air bar when the flotation height was adjusted. Keeping trailing edge slots open, pressure readings were recorded for four different gaps. This experiment attempts to test the replicability of results obtained in an earlier experiment (Pinnamaraju, 1992) conducted on the same lines. Plots were then generated for pressure versus distance.

Figures 14-17 show a comparison of plots generated by the present and earlier study respectively. As seen from the plots, pressure forces were higher near the slot and pressure forces decreased as the pressure tap moved away from the slot towards the trailing edge slot. Also, with increase in the gap between the air foil air bar and the rigid plate, the region of negative pressure forces increased near the trailing edge slot.

For gaps of 0.03 and 0.05 inches, there seemed to be considerable variation in the plots while for gaps of 0.07 and 0.10 inches, the general trend was almost the same but with some variation in the plots.

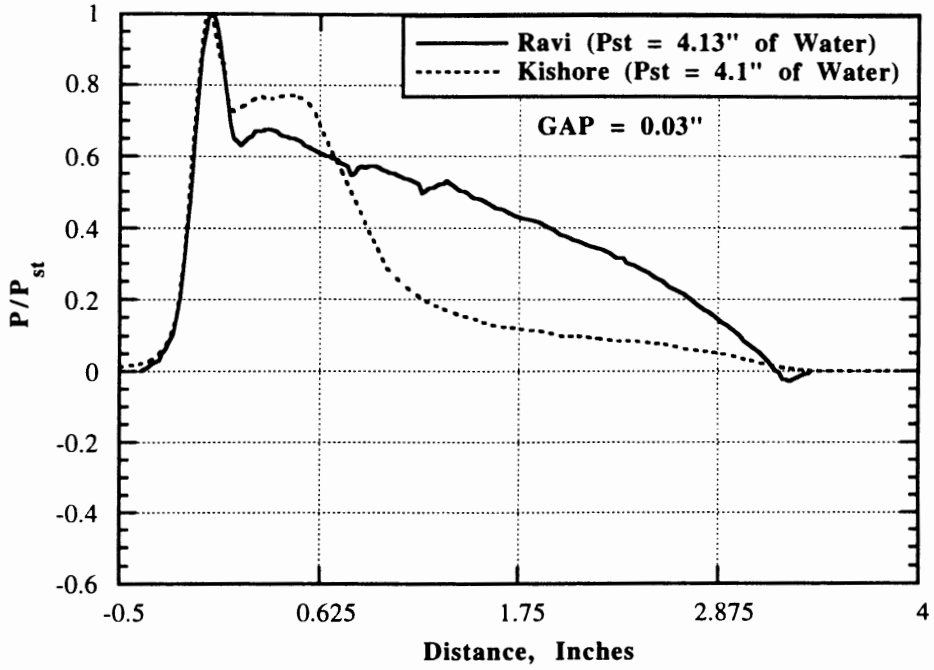

Figure14. Pressure Distribution of Air Foil (Trailing Edge Slot Open)

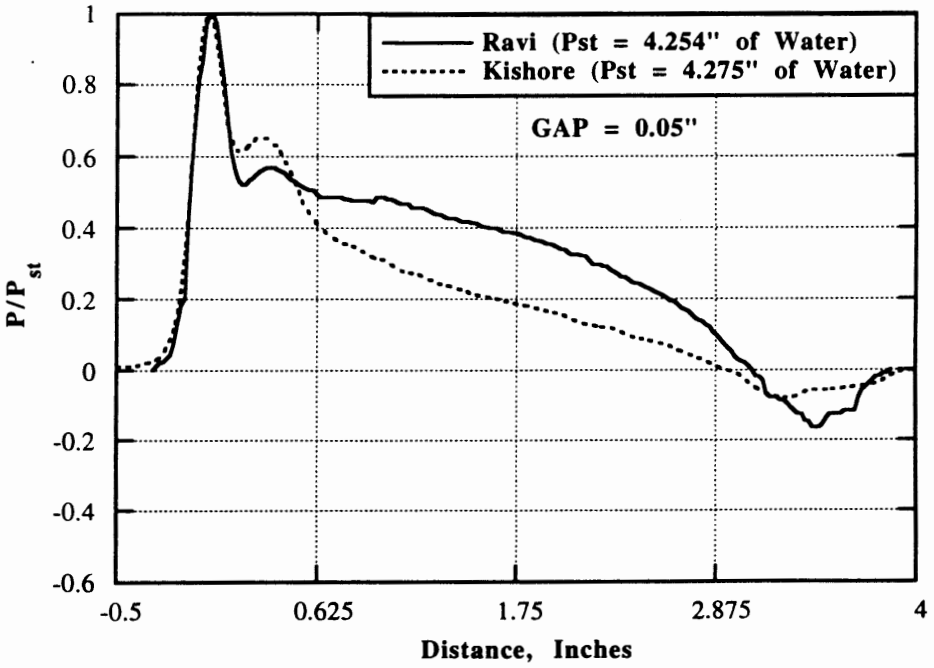

Figure15. Pressure Distribution of Air Foil (Trailing Edge Slot Open)

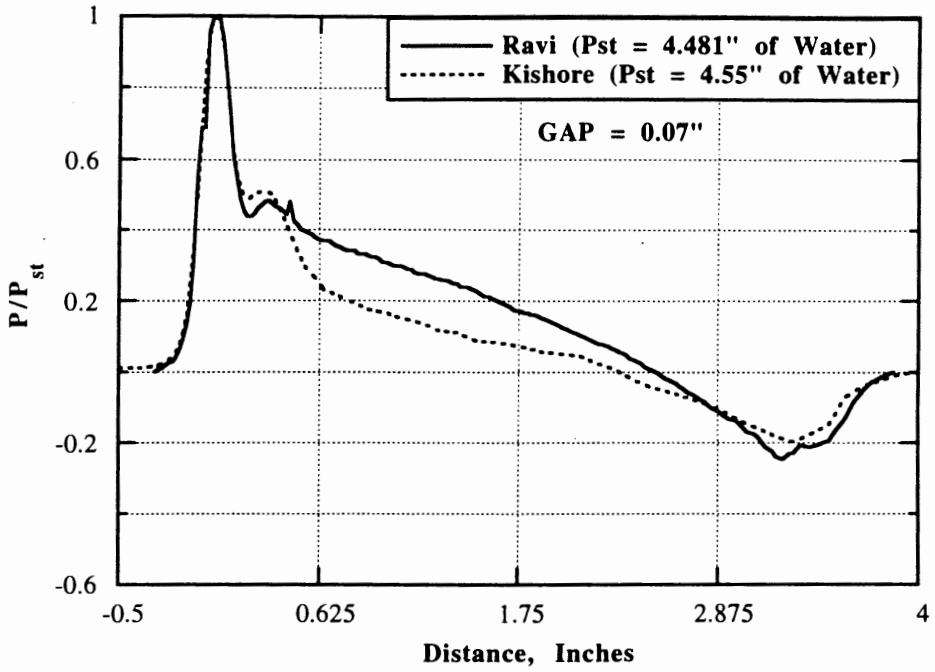

Figure 16. Pressure Distribution of Air Foil (Trailing Edge Slot Open)

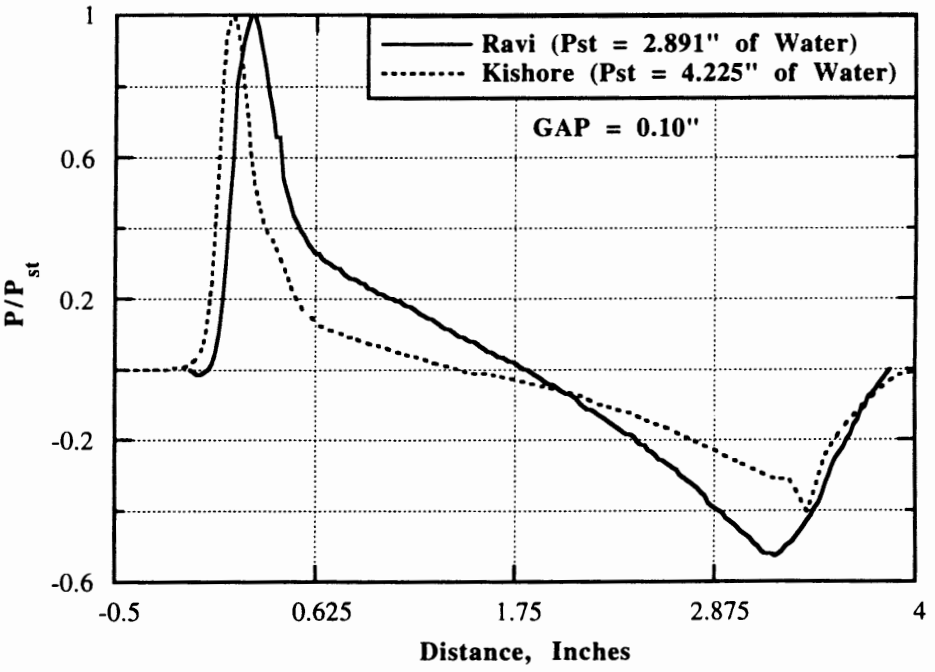

Figure 17. Pressure Distribution of Air Foil (Trailing Edge Slot Open)

The rigid plate was then rotated by 180 degrees and the experiments were repeated on the same lines to test the replicability of the results obtained in the present Setup I. Figures 18-20 show a comparison of the plots generated from readings obtained from Setup I and the Rotated Setup. These plots show that the general trend is almost the same and the variation in them, too, is minimal.

The total lift force was then found by integrating the area under the pressure versus distance curve. Plots were then generated for lift force versus gap. Figure 21 shows a comparison of lift forces with gap, for air foil air bar generated by the present and earlier study respectively.

As seen from Figure 21, for air foil air bar, the lift forces decrease drastically as the flotation height is increased for 0.0° tilt angle, exhibiting stable operation at small values of flotation height. For a negative slope, the lift forces decrease with increasing gap spacing. As the web moves away from the air bar, the tendency for it to continue moving diminishes. This acts to keep the web at the desired location.

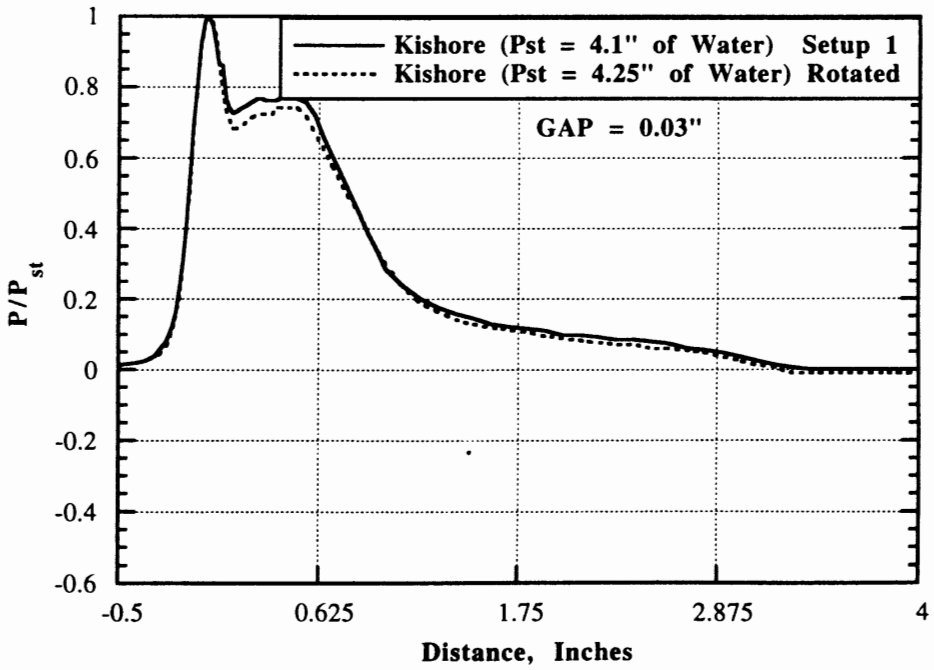

Figure 18. **Pressure Distribution of Air Foil (Trailing Edge Slot Open) for Two Setups.**

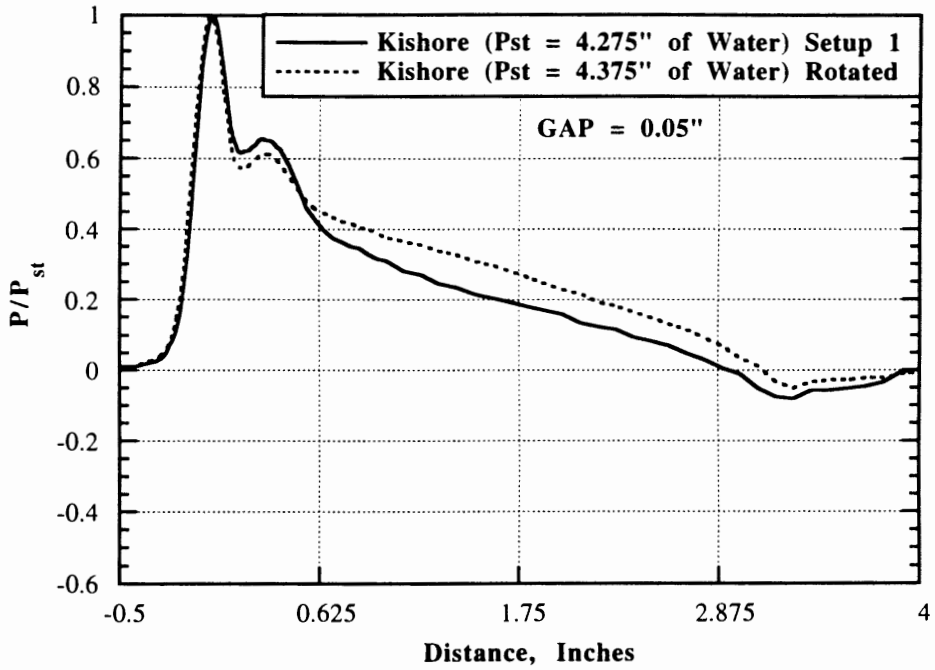

Figure 19. Pressure Distribution of Air Foil (Trailing Edge Slot Open) for Two Setups.

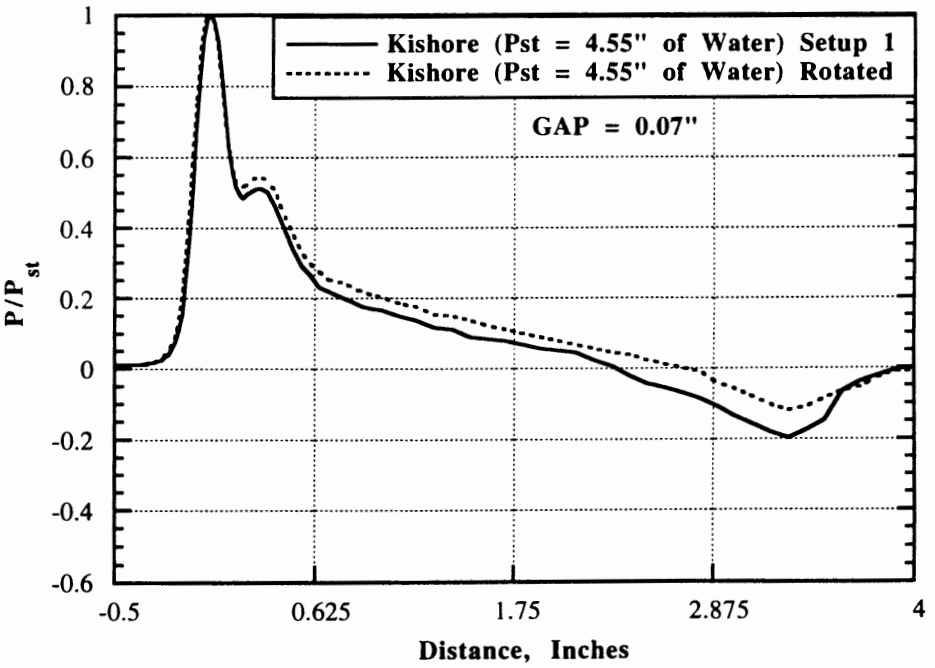

Figure 20. Pressure Distribution of Air Foil (Trailing Edge Slot Open) for Two Setups.

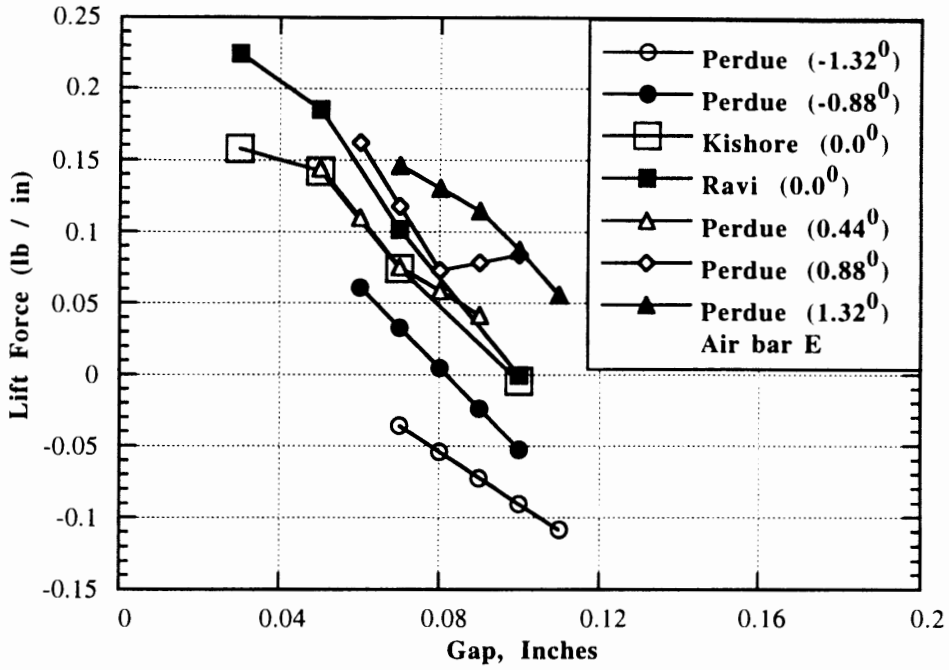

Figure 21. Comparison of Lift Forces for Airfoil Airbar (Trailing Edge Slots Open)

Perdue (1993), in his experiments tested the effects of machine-directional-tilt of the rigid plate on air foil type air bar. Figure 21 shows the lift forces versus gap spacing for various machine-directional-tilt angles. As seen from the figure, the lift forces increase with increase in the tilt angles. Figure also shows the lift forces obtained by the present and an earlier study at 0.0° tilt angle.

One of the persistent problems faced in the setting up of these experiments is the difficulty of adjusting the gap between the air bar and plate. This difficulty arises because of a rough edge due to a weld on the top of a commercial air bar. Thus the variation in lift forces is hypothesized to be due to slight errors in measurements and in the plate tilt in the machine direction. This problem was overcome with an increased number of gap measurement locations. When the tests conducted using the original setup and those conducted by using the reversed plate with an increased number of measurement stations are compared, we observe that the results are similar with little variation in them. Figures

18-20 show an agreement of the above mentioned tests with air foil type air bar. Tests were then carried out on pressure pad air bars with an increased number of gap measurement stations.

4.1.2 Pressure Pad Tube, Width = 3.6"

For the pressure pad tube, width = 3.6", pressure readings were taken from the center of the air bar, along its width, till the manometer read the atmospheric pressure. In this case, six sets of feeler gauges were placed along the length of the air bar. Keeping the pressure pad tubes center holes closed, pressure readings were taken for four different gaps and for three different gaps keeping its center holes open. This experiment attempts to test the replicability of results obtained in an earlier experiment conducted on the same lines. Plots were then generated for pressure versus distance.

Figures 22-25 show a comparison of plots for pressure pad tube, width = 3.6", center holes closed, that is, Air bar A, generated by the present and earlier study respectively. As seen from the plots, pressure forces are constant for most of the distance along the width of the pressure pad tube, but then increased to a maximum above the slot before decreasing to the atmospheric pressure. The variation in plots generated by the present and earlier study was small for gaps of 0.03" and 0.05" while it was considerable for 0.10" and 0.20".

Figure 29 shows a comparison of lift forces for air bar A. As seen from the figure, the total lift force decreased gradually with gap and had positive values for a wide range of gaps. The lift forces are much higher when compared to the air foil type. Also, the total lift forces obtained in the present experiment are higher than the ones obtained in an earlier experiment.

Figures 26-28 show a comparison of plots for pressure pad tube, width = 3.6" and center holes open, that is, Air bar B. As seen from the plots, pressure forces are maximum

at the center of the pressure pad tube. The pressure forces then decreased and maintained a constant value for most of the distance but then increased above the slot before decreasing to the atmospheric pressure. The variation in plots was small for gaps of 0.036" and 0.07" while it was considerable for 0.10".

Figure 29 also shows a comparison of lift forces for air bar B. As seen from the figure, the total lift force decreased gradually with gap. The total lift forces obtained in the present experiment are higher than the ones obtained in an earlier experiment.

For air bars A and B, the lift forces decreased gradually with increase in flotation height, indicating stable operation.

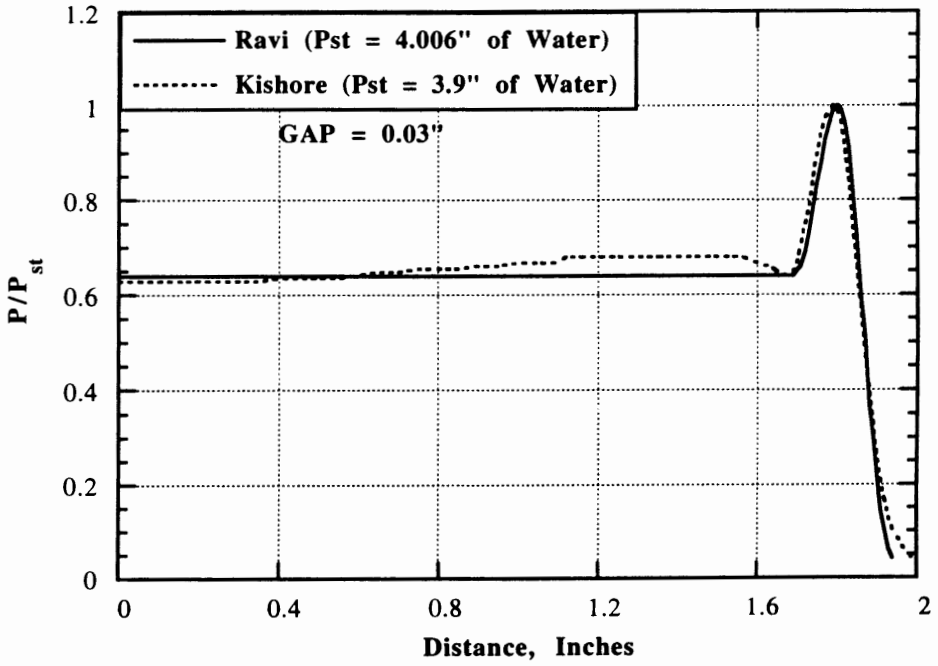

Figure 22 Effect of Gap on Pressure for PPT, W = 3.6". Center Holes Closed.

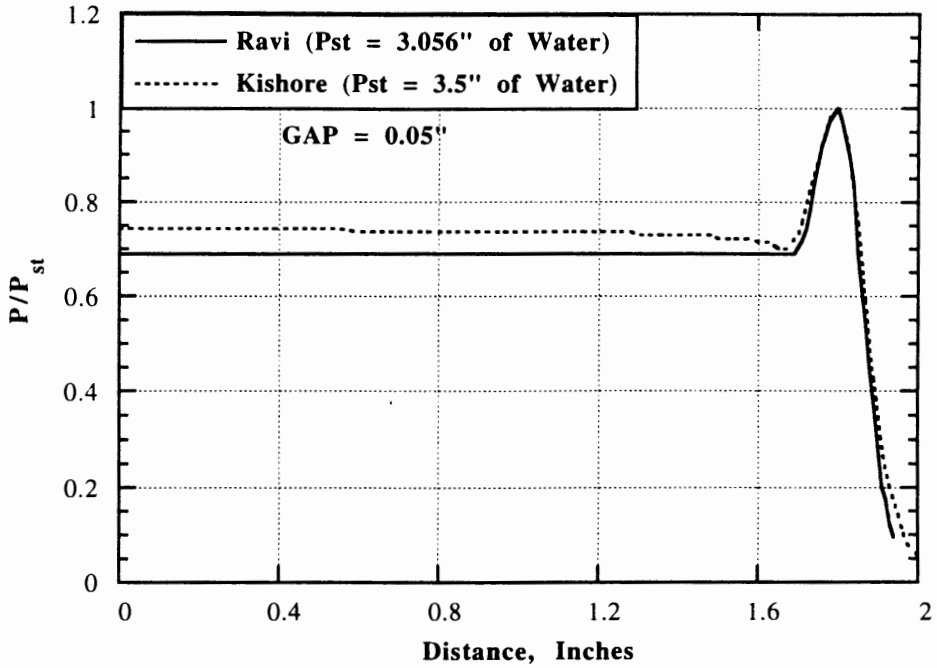

Figure 23. Effect of Gap on Pressure for PPT, W = 3.6". Center Holes Closed.

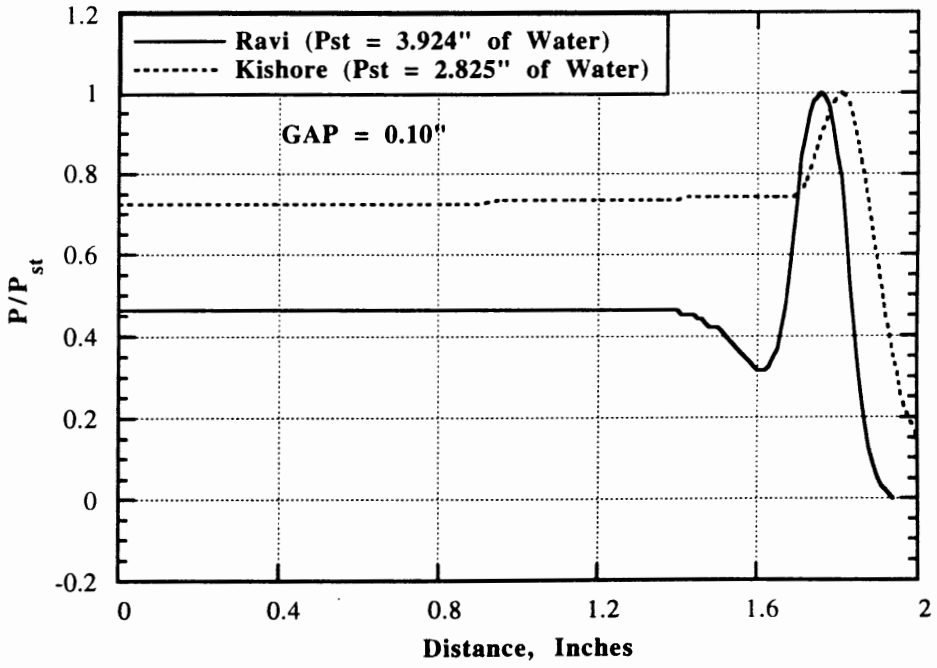

Figure 24. Effect of Gap on Pressure for PPT, W = 3.6". Center Holes Closed.

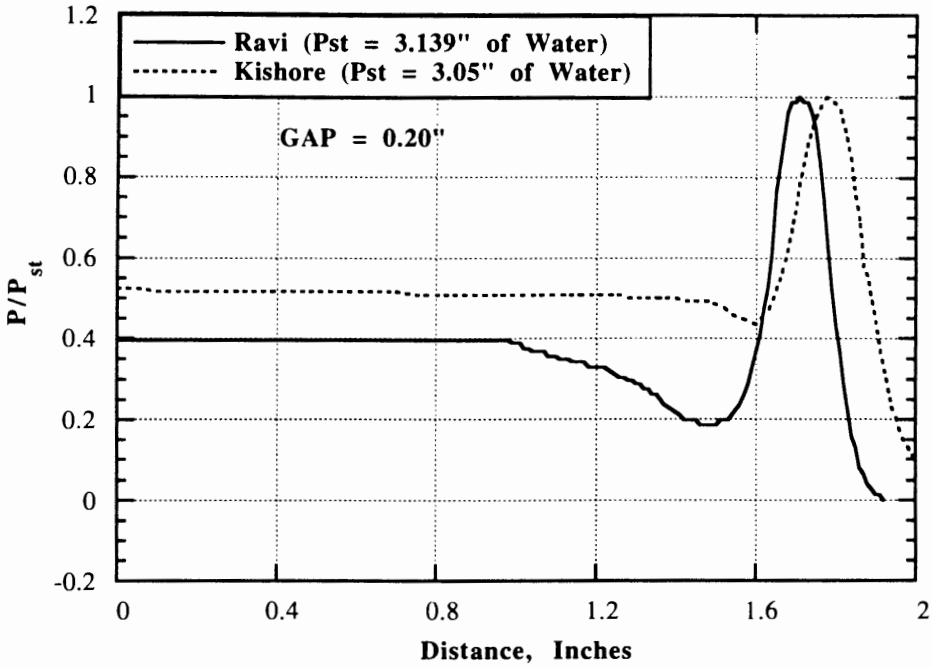

Figure 25. Effect of Gap on Pressure for PPT, W = 3.6". Center Holes Closed.

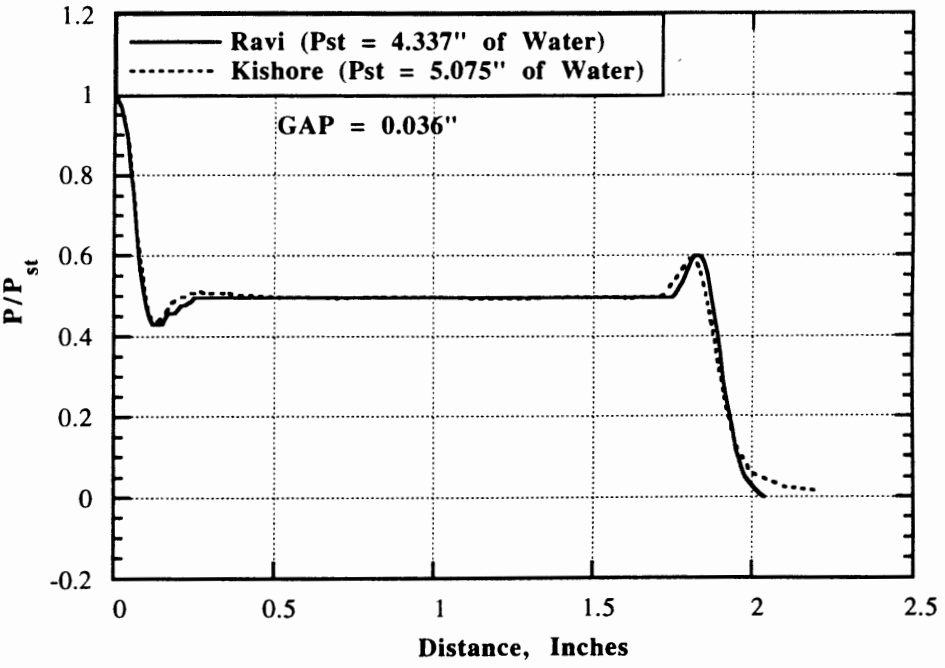

Figure 26. Effect of Gap on Pressure for PPT, W = 3.6". Center Holes Open.

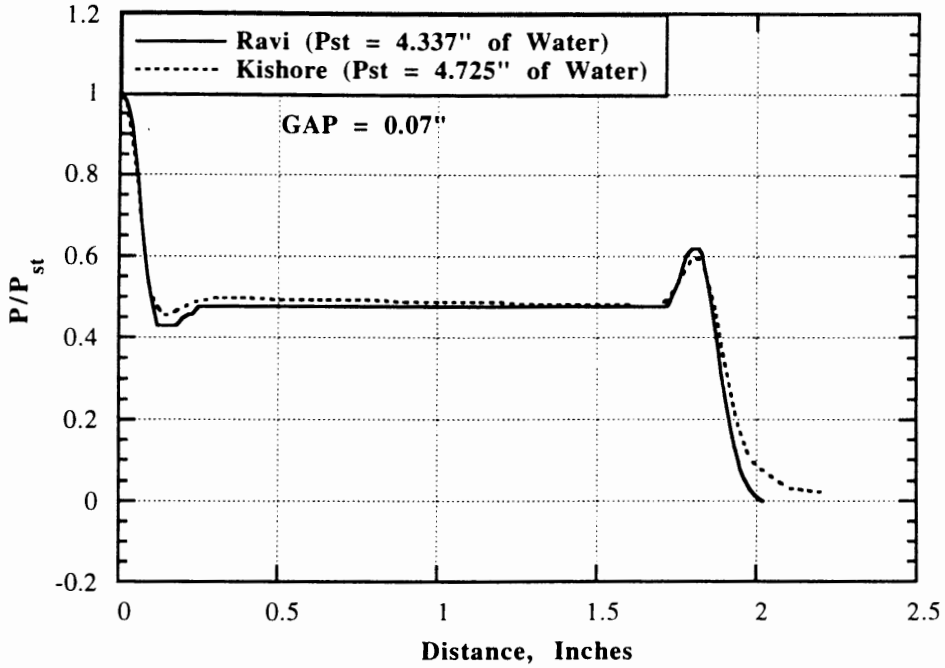

Figure 27. Effect of Gap on Pressure for PPT, W = 3.6". Center Holes Open.

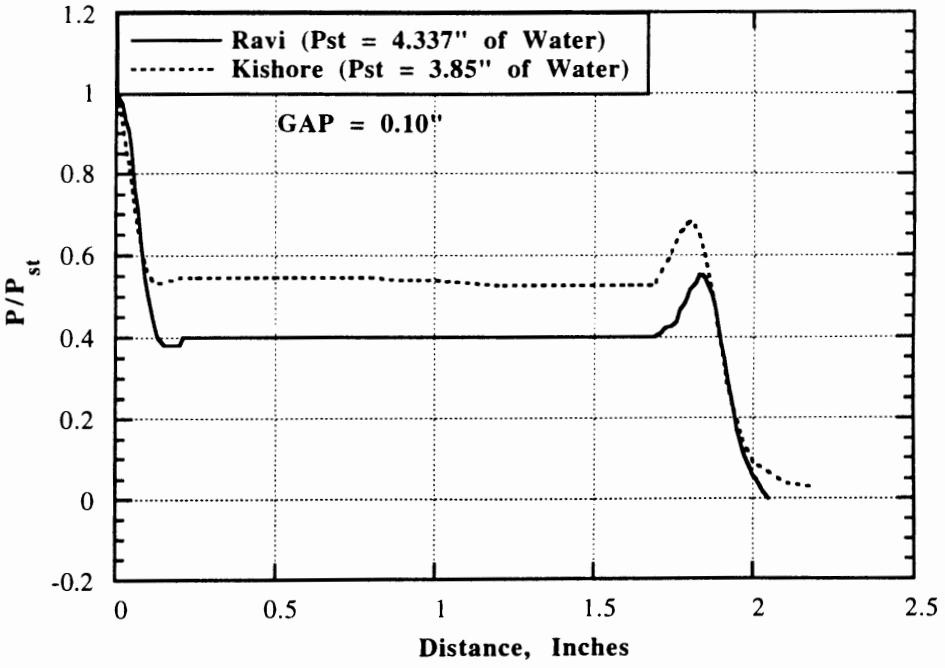

Figure 28. Effect of Gap on Pressure for PPT, W = 3.6". Center Holes Open.

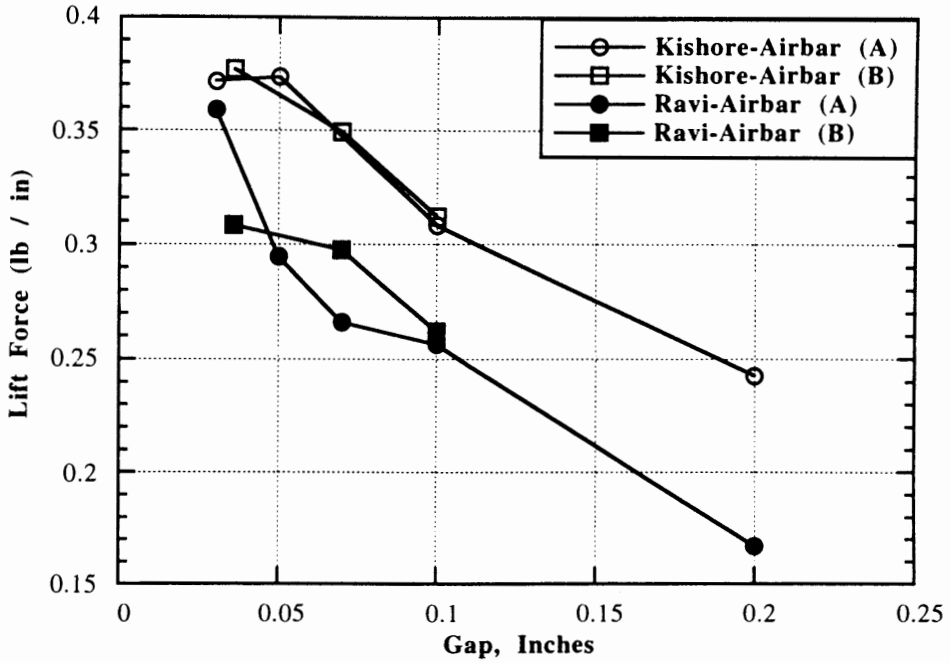

Figure 29. **Comparison of Lift Forces for PPT, W = 3.6"**

4.1.3 Pressure Pad Tube, Width = 5.0"

For the pressure pad tube, width = 5.0", pressure readings were taken in the same fashion as in the case of the pressure pad tube, width = 3.6". Pressure readings were taken for four different gaps keeping the center holes open in the first case and closed in the second case.

Figures 30-33 show a comparison of plots for the pressure pad tube, width = 5.0", center holes open, that is, Air bar C, generated by the present and earlier study respectively. As seen from the plots, the variation was small for gaps of 0.03" and 0.05", while it was considerable for 0.10" and 0.20".

Figure 38 shows a comparison of lift forces for air bar C. As seen from the figure, the total lift forces initially increased with increase in gap and then decreased. But, they maintained a positive value for a wide range of gaps. The regions of positive slope are

undesirable because it may cause static or dynamic instability. The web will want to fly off the air bar unless some other force influences its behavior. The total lift forces obtained in the present experiment are higher than the ones obtained in an earlier experiment.

Figures 34-37 show a comparison of plots for the pressure pad tube, width = 5.0", center holes closed, that is, Air bar D. They have the same trend as in the case air bar A. A comparison of lift forces for air bar D is obtained from Figure 38. As seen from the figure, the total lift forces decreased with increase in gap and had positive values for a wide range of gaps, indicating stability. Also, the lift forces obtained in the present experiment are higher than the ones obtained in the earlier experiment.

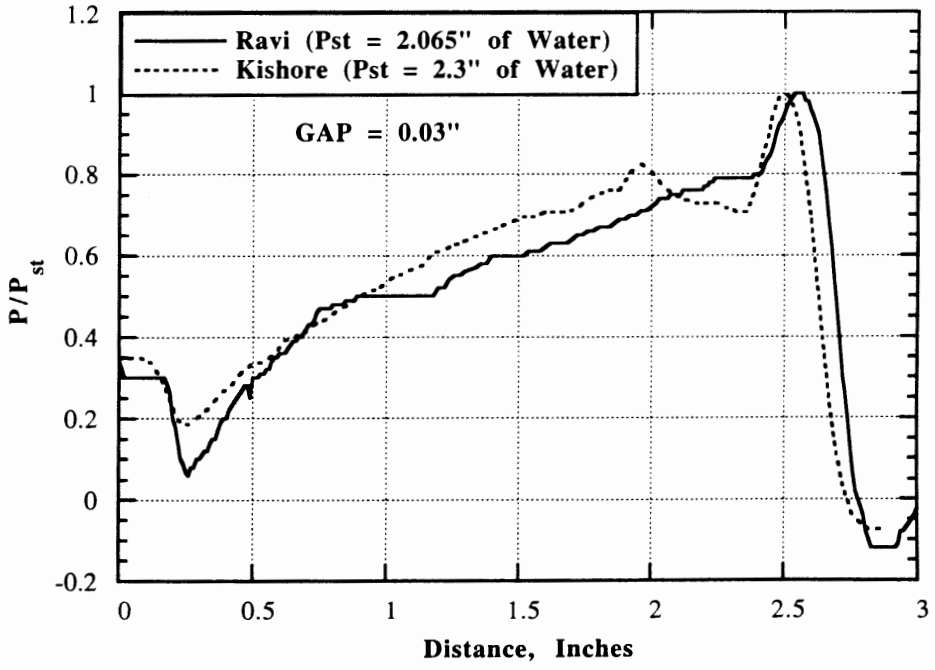

Figure 30. Effect of Gap on Pressure for PPT, W = 5.0". Center Holes Open.

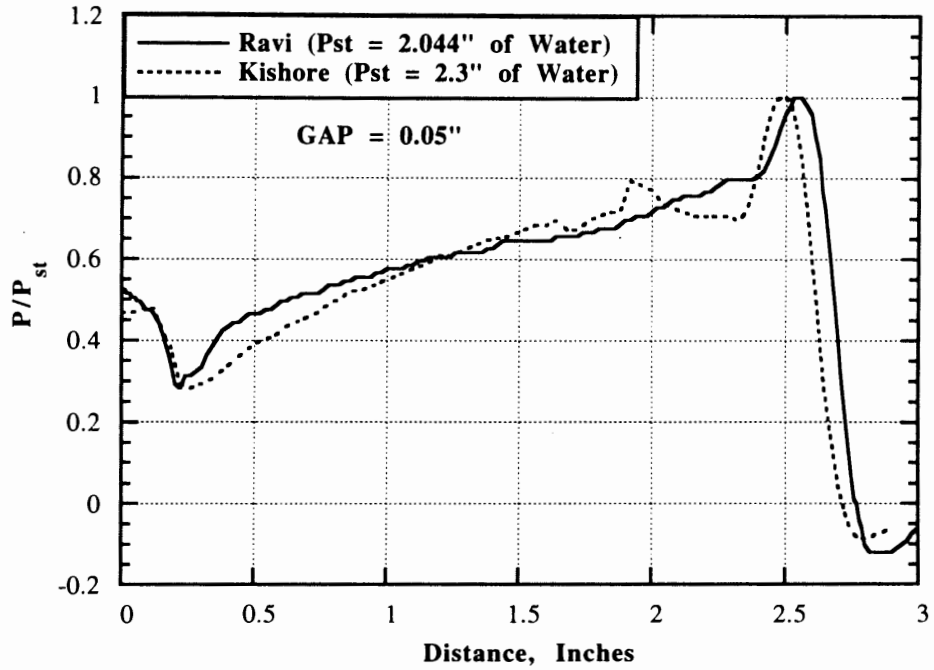

Figure 31. Effect of Gap on Pressure for PPT, W = 5.0". Center Holes Open.

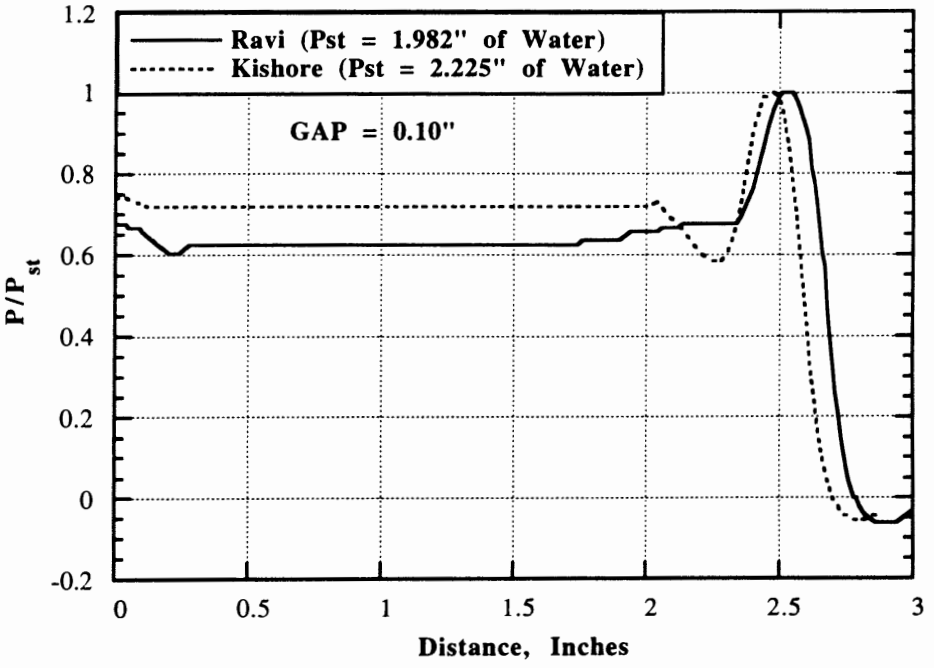

Figure 32. Effect of Gap on Pressure for PPT, W = 5.0". Center Holes Open.

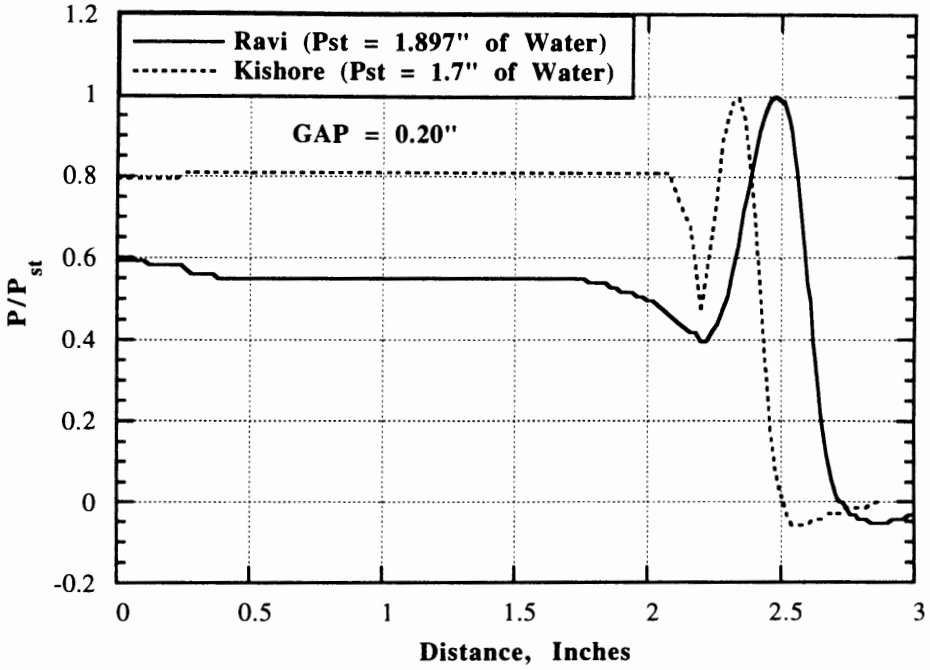

Figure 33. Effect of Gap on Pressure for PPT, W = 5.0". Center Holes Open.

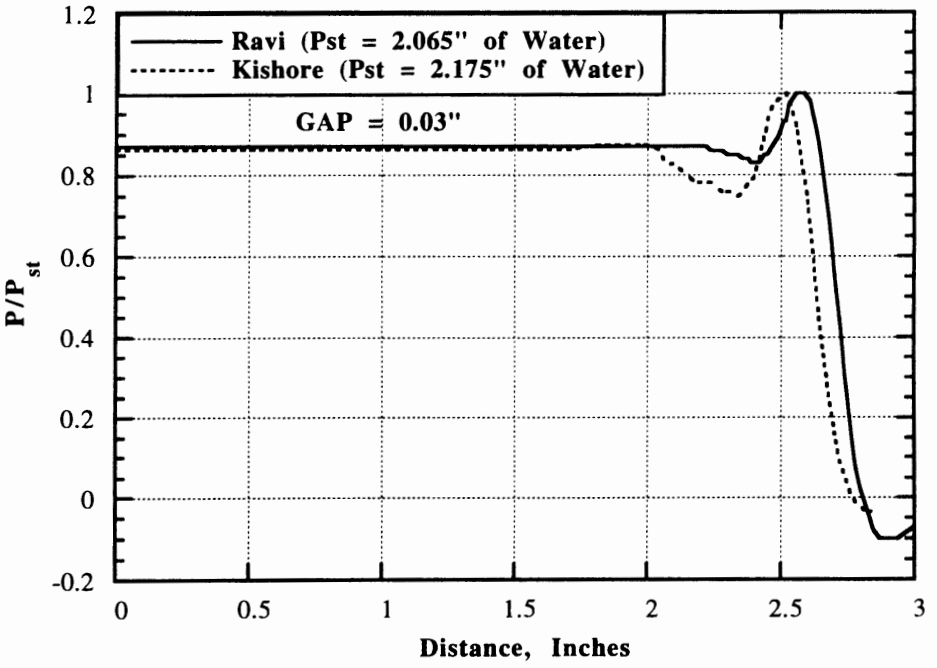

Figure 34. Effect of Gap on Pressure for PPT, W = 5.0". Center Holes Closed.

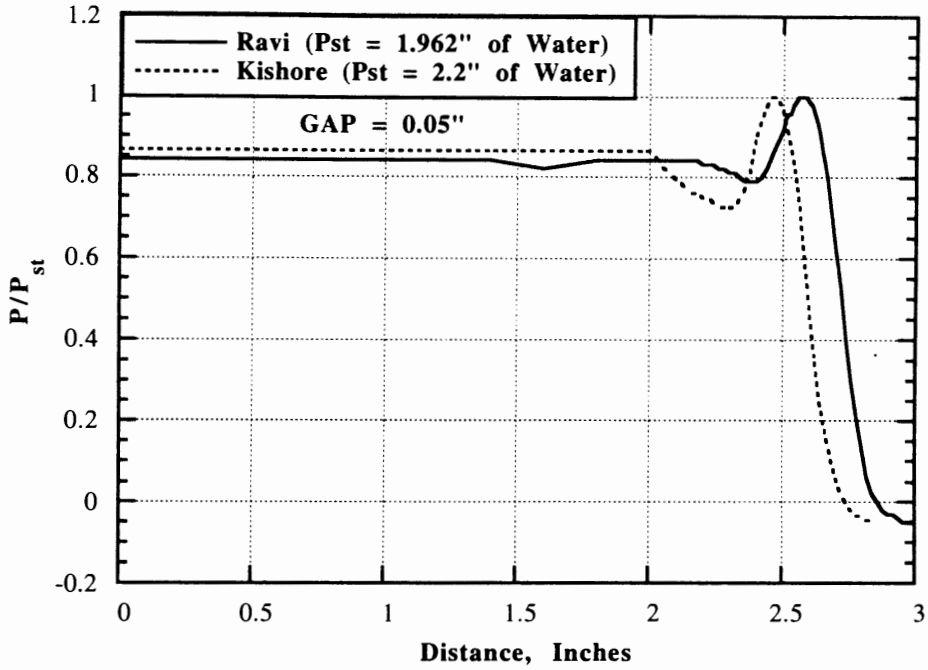

Figure 35. Effect of Gap on Pressure for PPT, W = 5.0". Center Holes Closed.

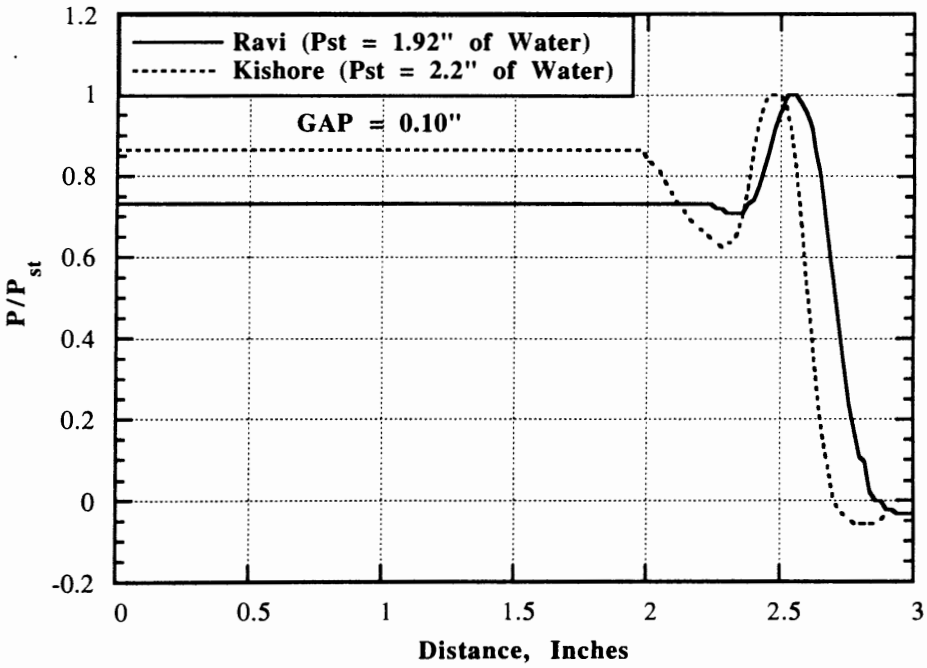

Figure 36. Effect of Gap on Pressure for PPT, W = 5.0". Center Holes Closed.

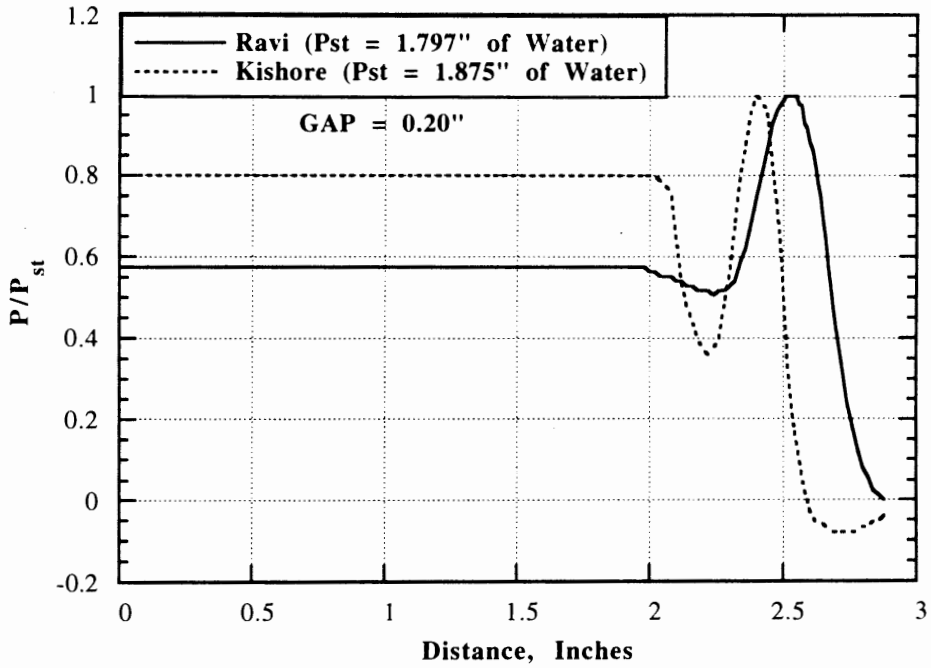

Figure 37. Effect of Gap on Pressure for PPT, W = 5.0". Center Holes Closed.

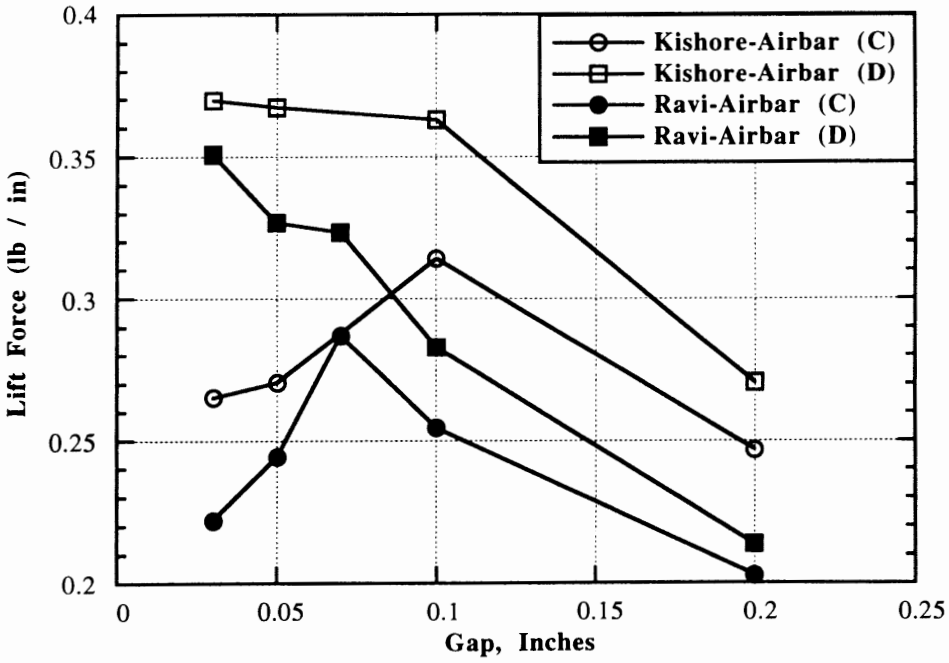

Figure 38. Comparison of Lift Forces for PPT, W = 5.0"

4.1.4 Comparison with Ground Effect Theory

The current test results were compared with the ground effect theory following the methods suggested in Moretti and Chang (1994). The first step is to define the equivalent values of jet width, jet angle, and jet velocity. The width of the jet exit is not uniform and the equivalent jet width is defined by the minimum value as shown in Figure 39.

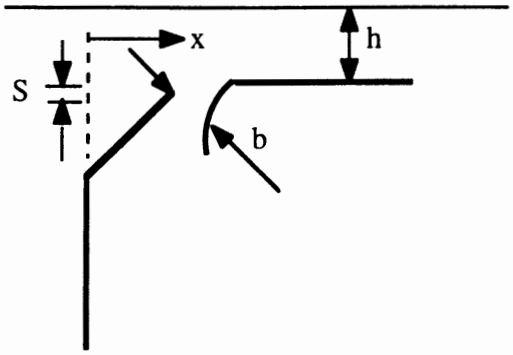

Figure 39.

The equivalent jet velocity was calculated by using

$$V_{jet} = \sqrt{(2 P_j / e)}$$

The jet angle is the quantity which is most uncertain. When the plate was removed, it was observed that the jet flow is attached to the surface of the air bar so that the angle is nearly zero. This is the phenomenon usually called "Coanda effect." Therefore, the angle could not be determined without the rigid plate. In order to determine the jet angle, the location of peak pressure was measured for various flotation heights. After defining those equivalent quantities, the uniform pressure inside the pressurized zone was calculated by using the equation

$$P_c = P_j (1 - \exp^{-2ß})$$

where, $ß = \frac{b (1 + \cos ø)}{h^*}$, $h^* = h + S$

and compared with the measured air pressure which is nearly uniform along the width of the air bar. Also, the theoretical total lift force is calculated by using the equation

$$F = P_c w + 2ebV^2_{jet} \sin\phi$$

From Figure 40, the average angle of the jet was found to be 73°. The equivalent jet velocity depends on the total (impact) pressure of the air relative to the atmospheric pressure. The total pressure could be measured before the jet formation, in the supply plenum, or after jet formation, at the stagnation point on the impingement plate. Using the former, we calculate too high a value for the jet flow and using the latter, too low a value (Figure 41). This indicates substantial losses due to viscous dissipation at the entrance of the jet as well as in the vicinity of the stagnation point. Figures 43-44 show a comparison of theoretical and experimental values of pressure and lift force repectively. If there were no losses then these values might lie on the 45° line.

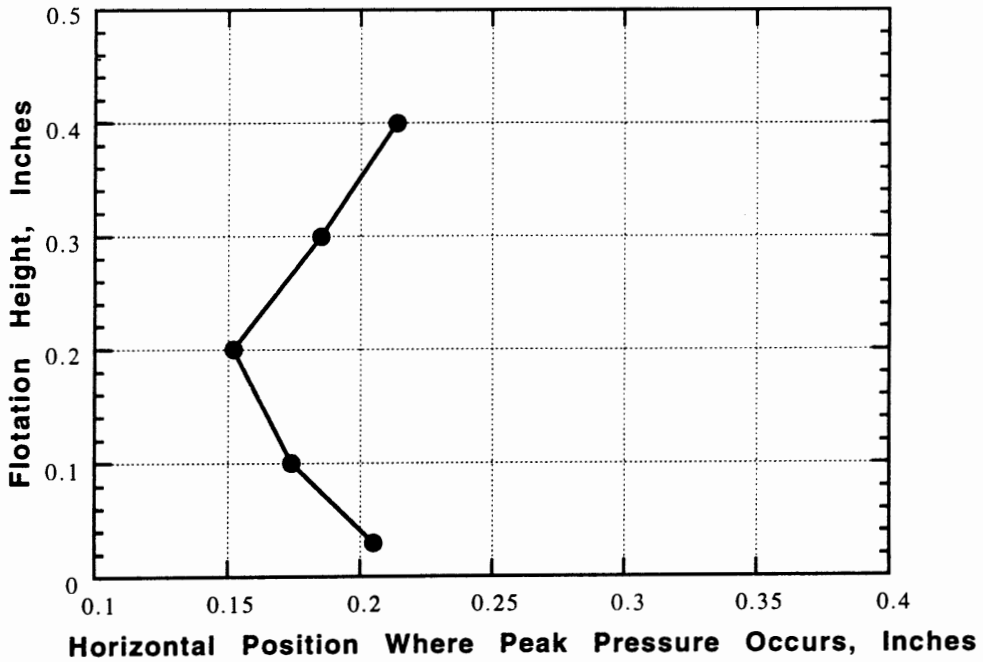

Figure 40. Horizontal Position of Peak Pressure for Various Flotation Heights

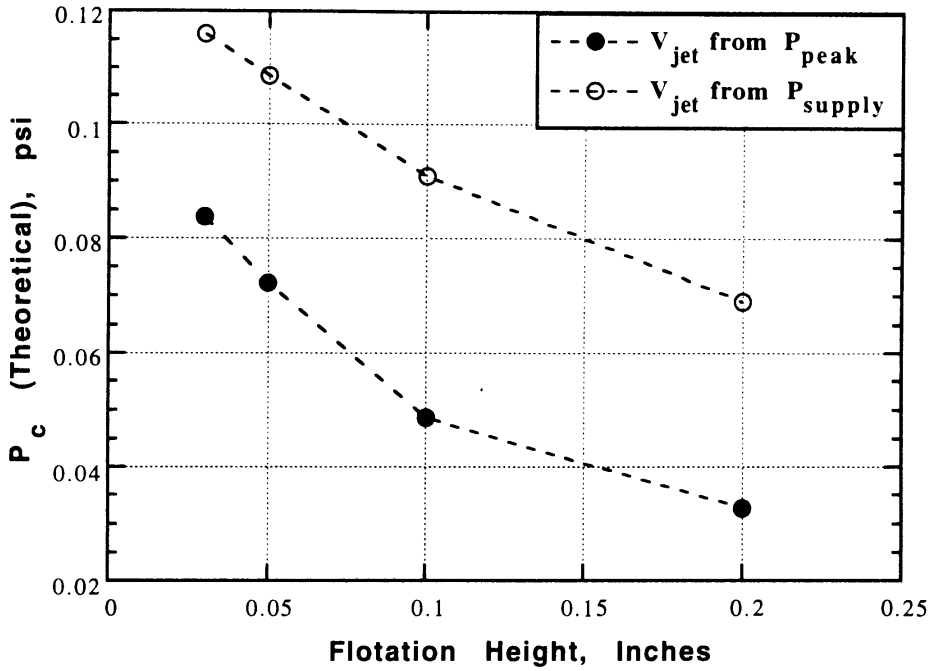

FIgure 41. Variation of Pc (Theoretical) with Flotation Height

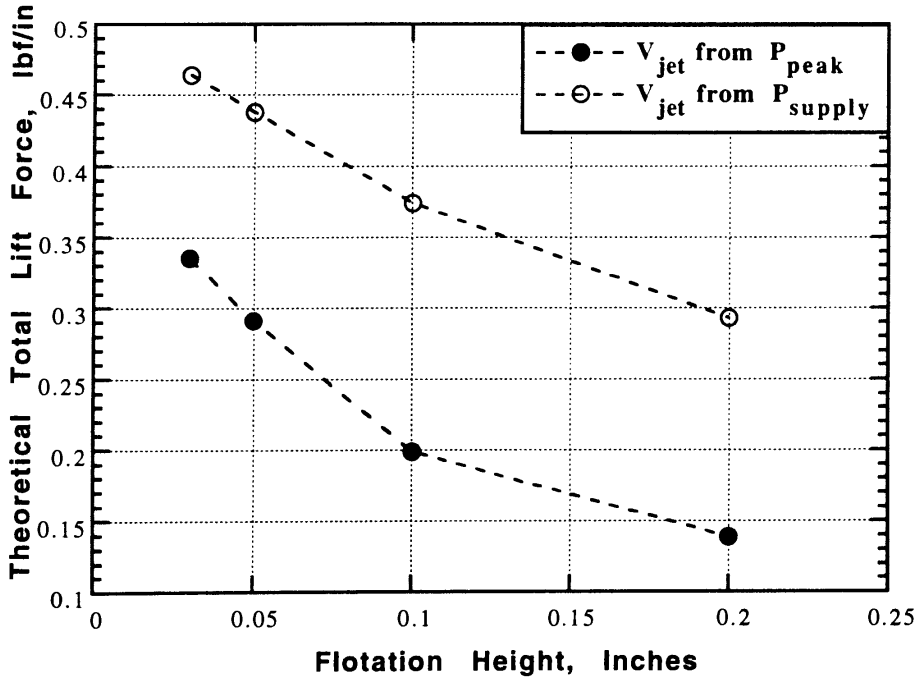

Figure 42. Variation of Theoretical Lift Force with Flotation Height

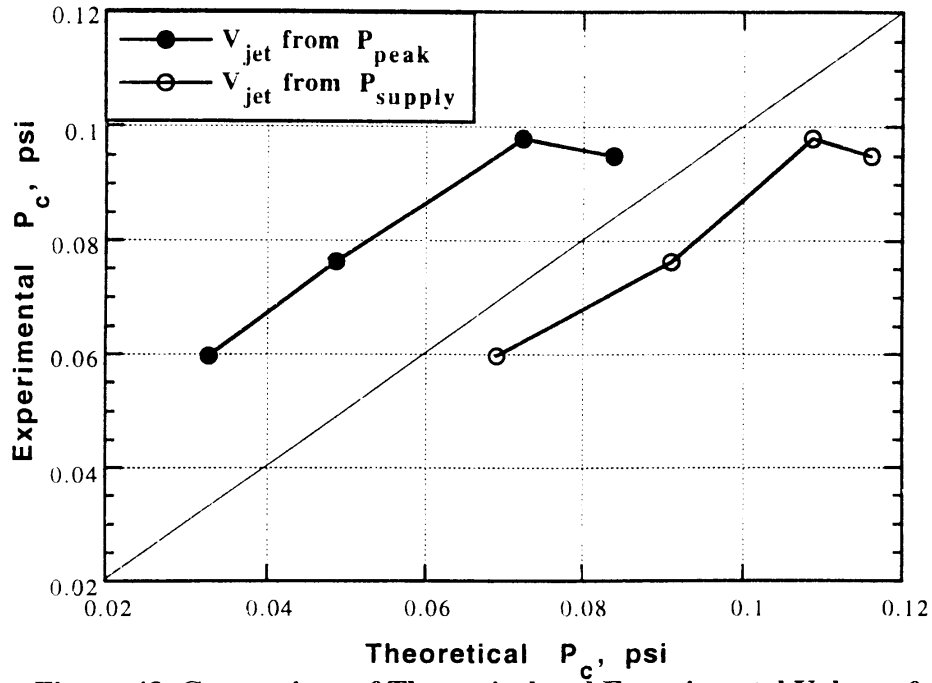

Figure 43. Comparison of Theoretical and Experimental Values of Pressure

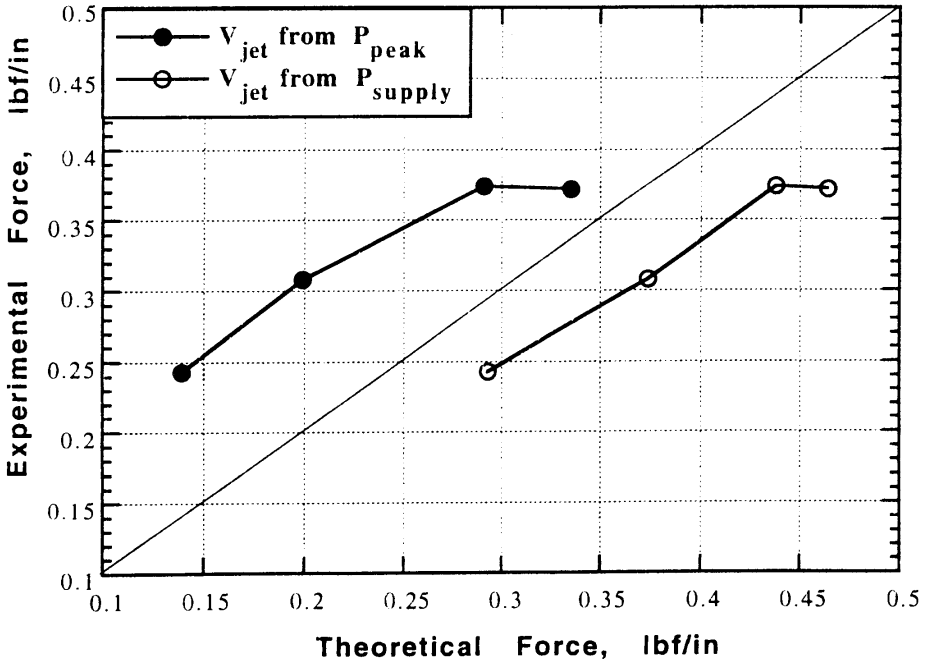

Figure 44. Comparison of Theoretical and Experimental Values of Force

4.2 Effects of Cross Machine Directional Tilt Angle

Perdue (1993), in his experiments tested the effect of machine directional tilt of the rigid plate on air foil type air bars. This experiment attempts to test the effect of cross machine directional tilt of the rigid plate on air bars. While checking the effect of cross machine directional tilt, pressure on the plate was read off nine pressure taps along the length of the plate (Y-direction) in inches of oil. The specific gravity of the oil used is 0.826.

The geometries of air bars that were used are :

(1) Pressure pad tube, width = 5.0", center holes closed.

(2) Air foil air bar with trailing edge slots open.

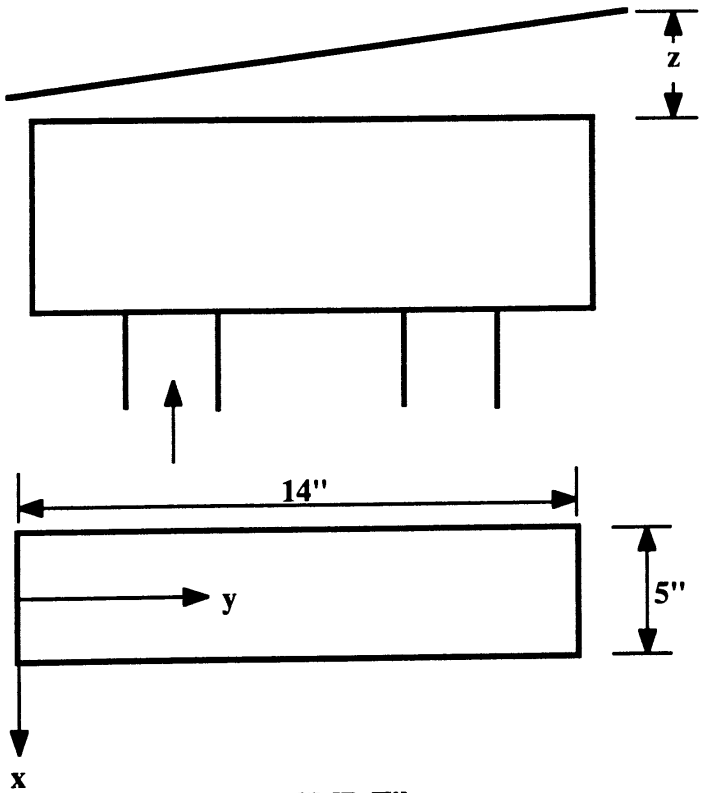

Figure 45. Setup for CMD Tilt

4.2.1 Pressure Pad Tube, Width = 5.0", Center Holes Closed

For this pressure pad tube, pressure readings were taken for four distances along the x-direction (Figure 45) and for four tilt angles. The tilt angle shown in figure 45 is positive in the clockwise direction. Also, air was supplied through the left approach tube as shown in figure. Figures 46-48 show the effect of pressure, with local gap z, for three tilt angles. As seen from the figures, the pressure is high at small gaps and decreases gradually with increase in local gap space. Changes in the tilt angle did not affect the pressure in any significant manner. As the pressure taps were moved from the center of the air bar towards the slot there was only a small variation in the observed pressure.

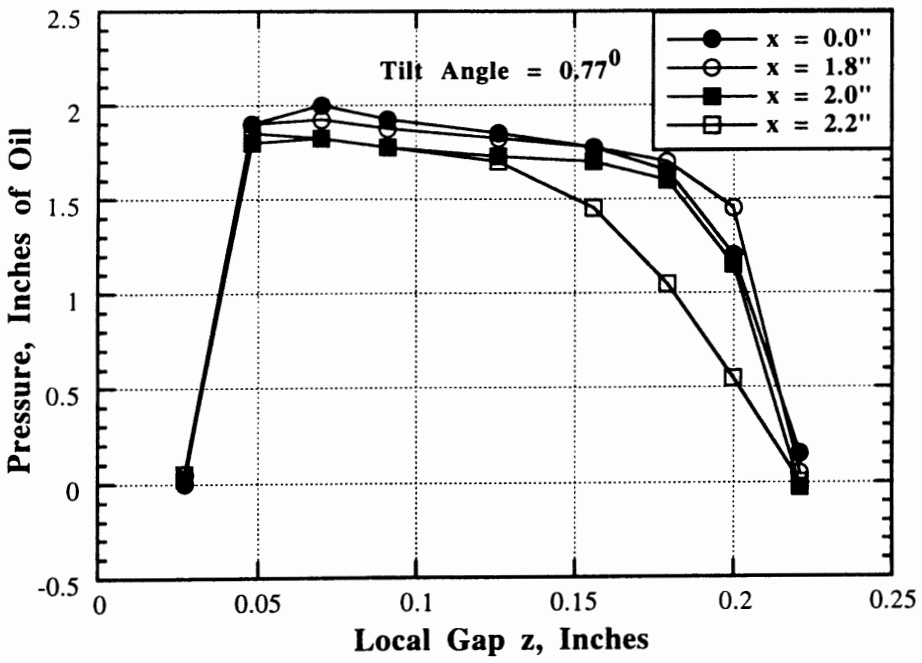

Figure 46. Variation of Pressure with Local Gap for PPT, W=5.0"

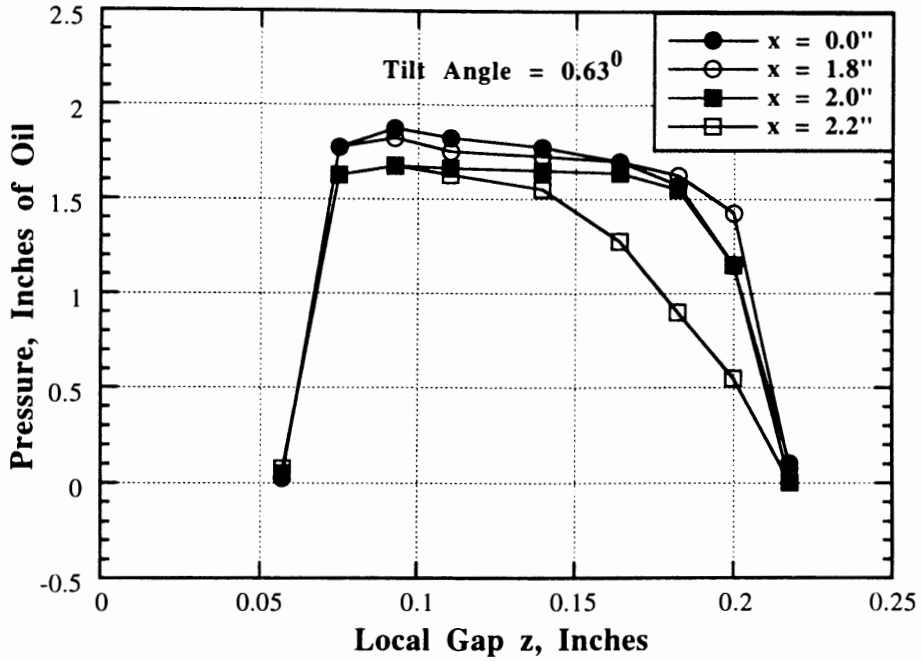

Figure 47. Variation of Pressure with Local Gap for PPT, W=5.0"

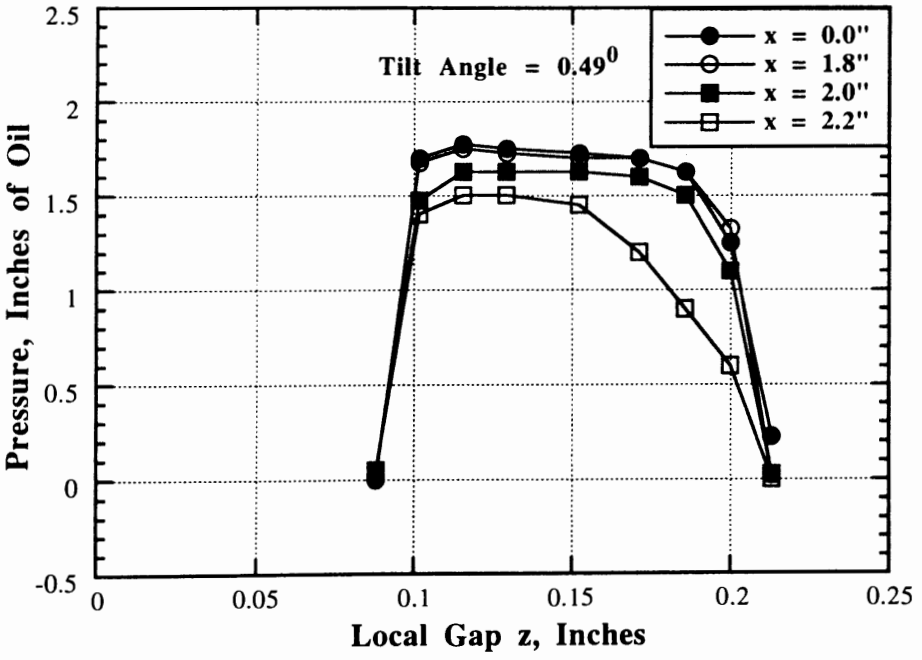

Figure 48. Variation of Pressure with Local Gap for PPT, W=5.0"

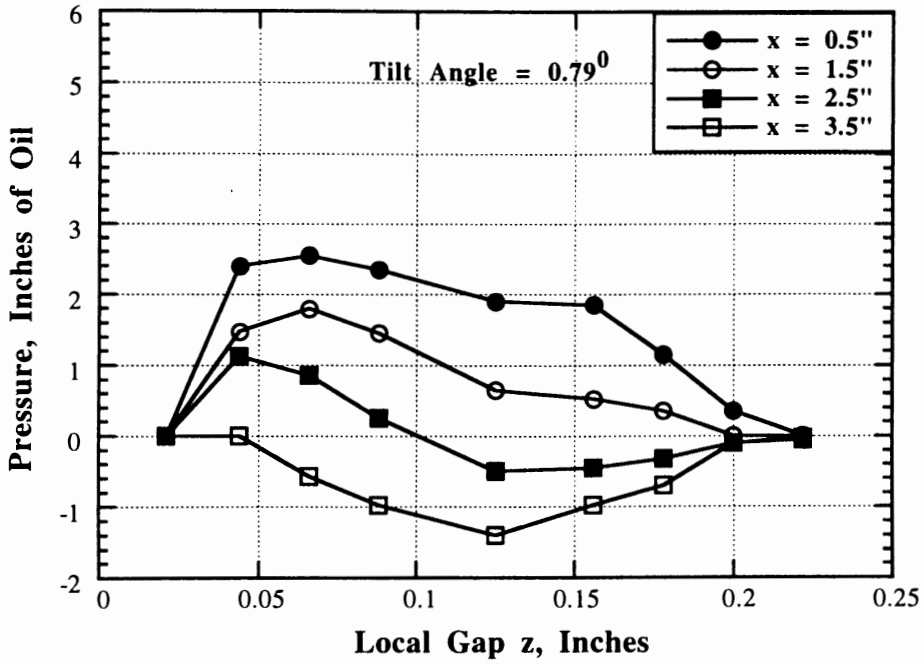

Figure 49. Variation of Pressure with Local Gap for Airfoil

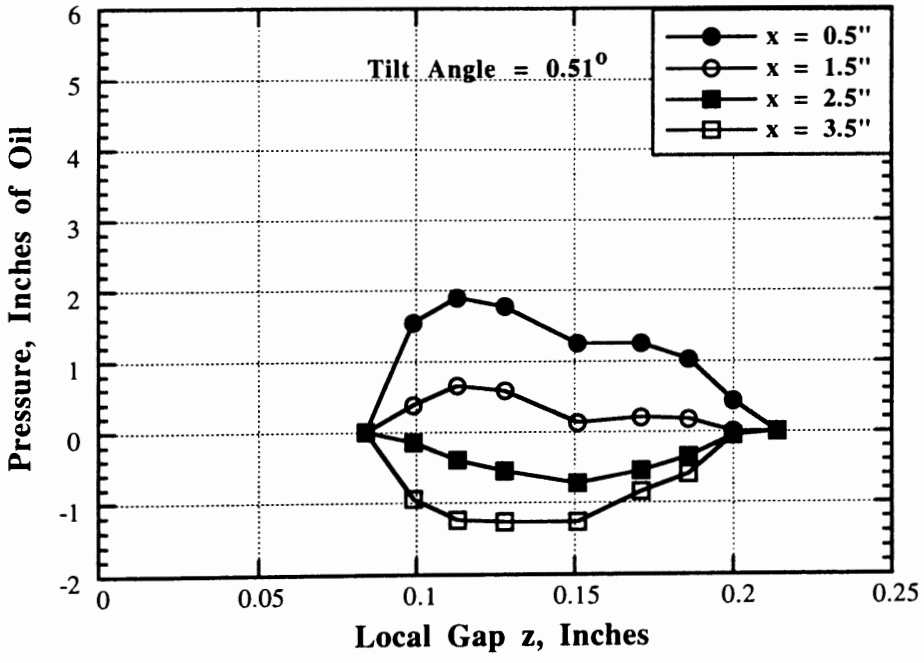

Figure 50. Variation of Pressure with Local Gap for Airfoil

Figures 49 and 50 show the effect of pressure on the local gap z, for two tilt angles for the airfoil air bar. As seen from the plots, the pressure decreased with increase in the gap spacing. Also, the region of negative pressure near the trailing edge slots increased.

The selection of the approach tube did not make much of a difference. As seen from figures 51 and 52, the pressure increased marginally when air was supplied through the right (that is, 2nd) approach tube. This was checked with the same setup, as shown in Figure 45. The only change was that the air was supplied through the right approach tube.

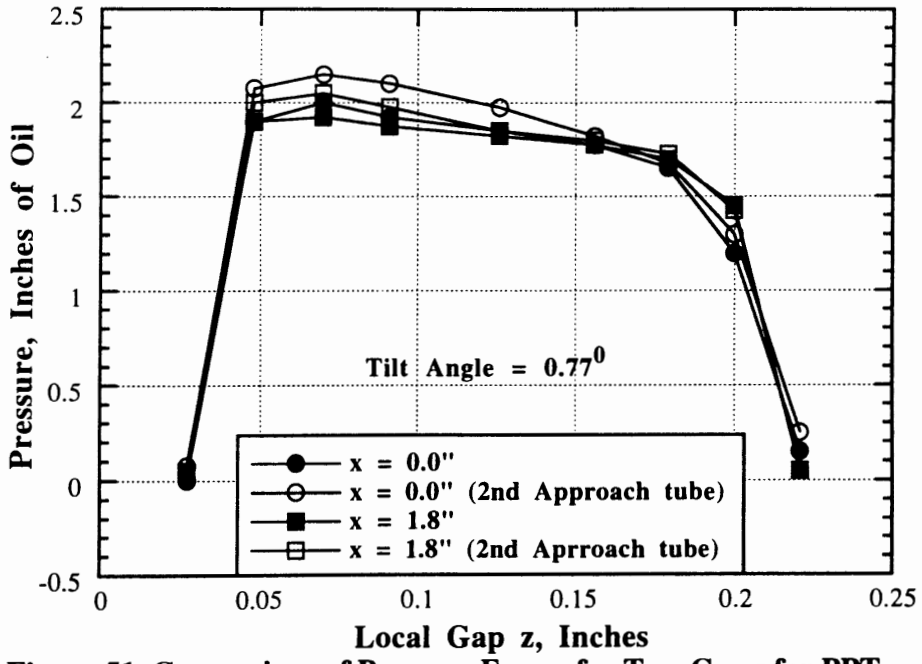

Figure 51. Comparison of Pressure Forces for Two Cases for PPT, W=5.0"

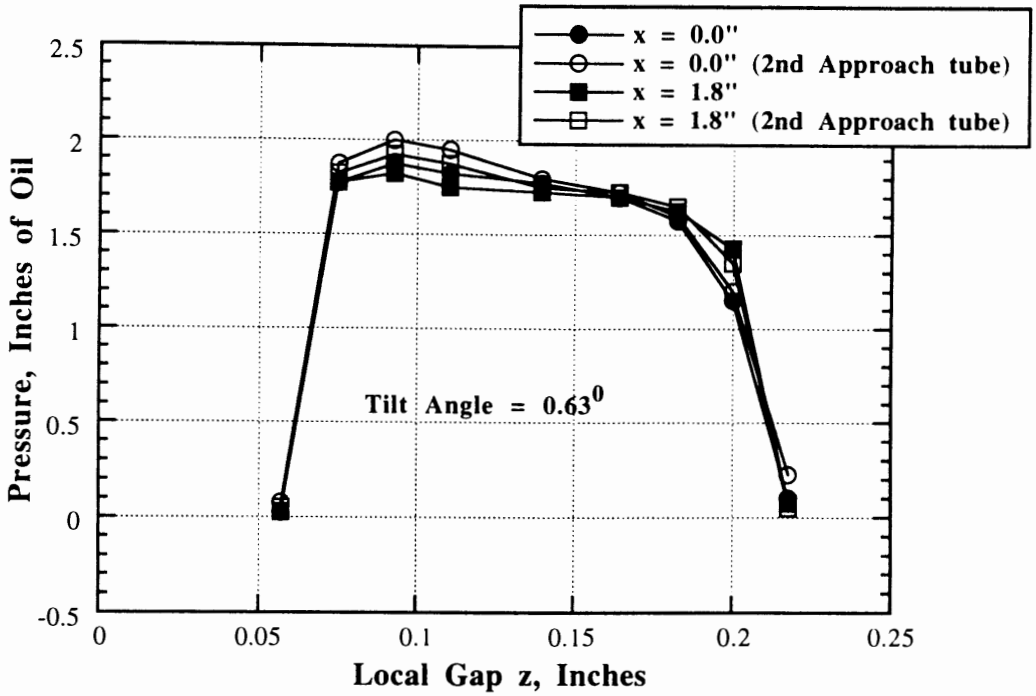

Figure 52. Comparison of Pressure Forces for Two Cases for PPT, W=5.0"

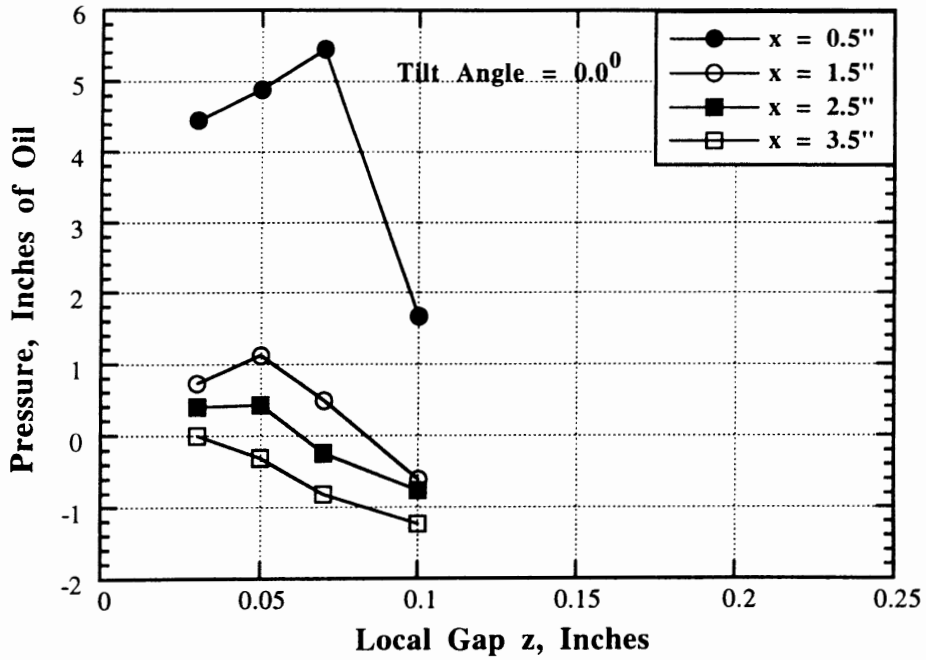

Figure 53. Variation of Pressure with Local Gap for Airfoil

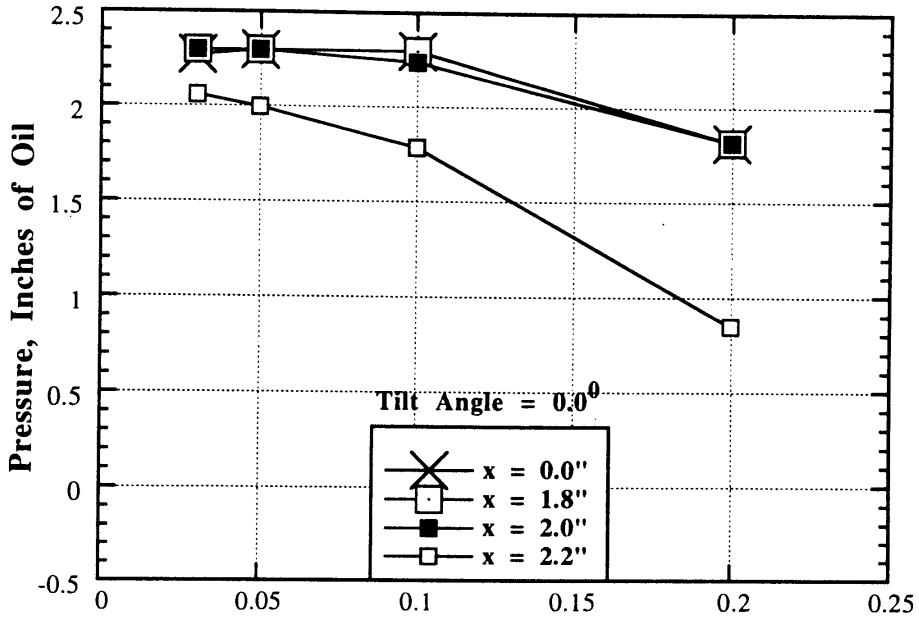

Figure 54. Variation of Pressure with Local Gap for PPT, W=5.0", Center Holes Closed

A comparison of pressure was made between the case of uniform flotation height and the cross machine directional tilt of the rigid plate for various distances along the width of the air bar.

Figures 53 and 49-50, show that for the same local flotation height with airfoil type air bar, the pressure for uniform flotation height case is higher than that for the tilted case near the slot. In addition, the region of negative pressure increases near the trailing edge slots, apparently due to complex three-dimensional flow patterns.

Figures 54 and 46-48, show that for the same local flotation height with pressure pad air bar D, the pressure for uniform flotation height case is higher than that for the tilted case. This shows that significant cross flows result from the tilt of the plate in the cross machine direction.

CHAPTER V

SUMMARY AND CONCLUSIONS

The aerodynamic characteristics of an air foil air bar and two pressure pad air bars have been experimentally studied. The web was modeled as a flat plate. First, the effects of flotation height were measured and the results were compared with the ones obtained by Pinnamaraju. Second, the effects of cross-machine-directional tilt angle were measured. The measured local pressures were compared with the results for the case of uniform flotation height. Third, the measured pressure distributions and the total aerodynamic forces on the rigid web were compared with the ground-effect-machine theory. From this study the following conclusions were obtained.

(1) For the air foil air bar, the lift forces decrease drastically as the flotation height is increased, exhibiting strongly stable operation at small values of flotation height. The lift forces obtained in the present experiment are lower than the ones obtained by Pinnamaraju; the earlier work showed the effect of a very slight error in plate tilt, which has been overcome in the present study through the use of an increased number of gap measurement locations.

(2) For the pressure pad air bar A (defined on p. 13) and the pressure pad air bar B (defined on p. 14), the lift forces decrease more gradually with increase in the flotation height, indicating stable operation.

(3) For the pressure pad air bar C (defined on p. 14), the lift forces initially increase and then decrease with increase in flotation height. The region of positive slopes is undesirable because it may cause static or dynamic instability.

(4) For the pressure pad air bar D (defined on p. 15), the lift forces decrease with increase in the flotation height, indicating stability. The lift forces for pressure pad air bars obtained in the present experiment are higher than those obtained in an earlier study since tests were carried out with a greater number of gap measurement stations. So the errors in plate tilt were minimal. Thus these results are more reliable.

(5) For the same local flotation height with the pressure pad air bar D (defined on p. 15), the pressure for the uniform flotation height case is higher than that for the tilted case. This shows that significant cross flows result from the tilt of the plate in the cross machine direction. For the same local flotation height with air foil air bar, the pressure for uniform flotation case is higher than that for the tilted case especially near the slot. In addition, the region of negative pressure increases near the trailing edge slots, apparently due to complex three-dimensional flow patterns.

(6) The important design or operating variables for a pressure pad air bar that determines its aerodynamic characteristics are the jet width, jet angle, jet velocity, and the width of the air bar (distance between the two slots) (pp. 34-35).

(7) The ground-effect theory (pp. 5-6) can be useful in predicting the aerodynamic characteristics of pressure pad air bars if the equivalent values of the above four variables are properly defined.

(8) Since machine-direction tilt has strong effects on pressure distribution, future work should include work with flexible webs. An exploratory experiment has shown that it is possible to determine flexible web contours optically, and obtain pressure differences from web curvature.

CITED WORKS

Charles, A. R., and Donald, W. L., " The Use of Airfoils in Drying Coated Paper," Tappi Journal 56 (4) (1973): 86-89.

Davies, M.J., and Wood, D.H., " The Basic Aerodynamics of Flotation," Journal of Fluids Engineering 105 (1983): 323-328.

Fraser, W.R., "Air Flotation Systems: Theoretical Considerations & Practical Applications," Paper, Film & Foil Converter May 1983, 162.

Gary, L.B., " Applications of Floater Dryers to the Paper Industry," Tappi Journal 59 (4) (1976): 92-96.

Hwang, C.J., and Liu, J.L., " Numerical Study of Two-Dimensional Impinging Jet Flowfields," AIAA Journal 27 (7) (1989): 841.

Kataoka, K., "Optimal Nozzle to Plate Spacing for Convective Heat Transfer in Nonisothermal, Variable Density Impinging Jets," Drying Technology 3 (2) (1985): 235-254.

Krizek, F., " Impinging Jet Systems to Support and Dry Paper," Drying Technology 4 (2) (1986):271-294.

Mair, W.A., " The Physical Principles of HoverCraft," Journal of the Royal Aeronautical Society, 1964: 5-13.

Moretti, P.M., and Chang, Y.B., " Ground-effect theory and its application to air flotation devices," Internal Report of WHRC, 1994.

Obrzut, J.J., " Coil Coaters Float Strip Through Ovens," Iron Age November 1976, 31-33.

Page, R.H., and Seyed-Yagoobi, J., " A New Concept for Air or Vapor Impingement Drying," Tappi Journal September 1990: 229-234.

Perdue, D., " Lateral Stability Investigation of Air Bar and Web Interaction for Use in Flotation Ovens," M.S. thesis, Oklahoma State University, 1993.

Pinnamaraju, Ravi, " Measurements on Air Bar/Web Interaction for the Determination of Lateral Stability of a Web in Flotation Ovens," M.S. report, Oklahoma State University, 1992.

VITA

SAI KISHORE V. NISANKARARAO

Candidate for the Degree of

Master of Science

Thesis: AN EXPERIMENTAL STUDY OF AERODYNAMIC FORCES OF AIR BARS

Major Field: Mechanical Engineering

Biographical:

Personal Data: Born in Hyderabad, Andhra Pradesh, India, December 4, 1969, son of Rudra Murthy Nisankararao and Padmavathy Mettu.

Education: Graduated from Bharatiya Vidya Bhavans Public School, B.H.E.L, Hyderabad, India, 1987; received Bachelor of Engineering in Mechanical Engineering from Madras University, Madras, India, in August 1991; completed requirements for the Master of Science Degree at Oklahoma State University in May, 1994.

Professional Experience: Graduate Research Assistant, Department of Mechanical Engineering, Oklahoma State University, August, 1993, to May, 1994.